

# Journal Pre-proof

Focal Scleral Nodule - A New Name for Solitary Idiopathic Choroiditis / Unifocal Helioid Choroiditis

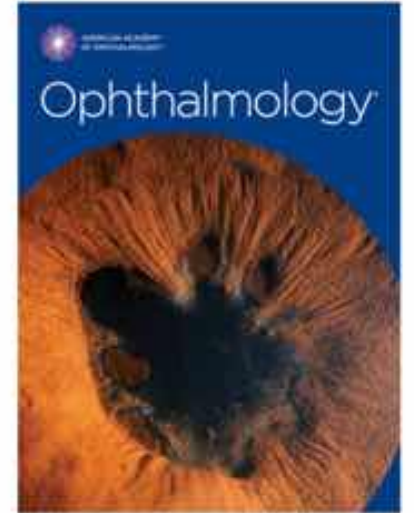
Adrian T. Fung, Sebastian M. Waldstein, Orly Gal-Or, Marco Pellegrini, Chiara Preziosa, Jerry A. Shields, R. Joel Welch, Rosa Dolz-Marco, David Sarraf, Aaron Nagiel, Robert Lalane, Jesse J. Jung, Nicola G. Ghazi, Prithvi Ramtohum, Jennifer J. Arnold, Yoichi Sakurada, Netan Choudhry, Chandrakumar Balaratnasingam, K. Bailey Freund, Carol L. Shields

PII: S0161-6420(20)30396-1

DOI: <https://doi.org/10.1016/j.ophtha.2020.04.018>

Reference: OPHTHA 11213

To appear in: *Ophthalmology*



**Purpose:** To evaluate multimodal imaging findings of solitary idiopathic choroiditis (SIC, also known as **unifocal helioid choroiditis**) to clarify its origin, anatomic location, and natural course.

**Design:** **Multicenter** retrospective observational case series.

**Participants:** **63** patients with SIC in one eye.

**Results:** Mean age at presentation was  $56 \pm 15$  years (range, 12-83 years). Mean follow-up duration in 39 patients was  $39 \pm 55$  months (range, 1 month to 25 years). The lesions measured a mean of  $2.4 \times 2.1$  mm in basal diameter, were located inferior (64%) or nasal to the optic disc and appeared yellow in color (53%). There were no systemic associations. The lesions all appeared as an elevated subretinal mass, with OCT demonstrating all lesions to be confined to the sclera, not the choroid. On OCT the deep lesion margin was visible in 12 eyes with a mean lesion thickness of 0.6 mm. Overlying choroidal thinning or absence was seen in 95% (mean choroidal thickness,  $28 \pm 35$  microns). Mild subretinal fluid was observed overlying the lesions in 9 patients (14%). Retinal pigment epithelial (RPE) disruption and overlying retinal thinning was observed in 56% and 57%, respectively. OCTA was performed in 13 eyes and demonstrated associated choroidal and lesional flow voids. Four lesions (6%) were identified at the macula, leading to visual loss in one patient. One lesion demonstrated growth and another lesion showed spontaneous resolution.

**Conclusions:** In this largest series to date, multimodal imaging of SIC demonstrated a scleral location in all cases. The yellow/white clinical appearance may be related to scleral unmasking from atrophy of overlying tissues. Additional associated features included documentation of deep margin on swept-source OCT, trace subretinal fluid in a few cases, and OCTA-evidence of lesional flow voids. Due to the scleral location of this lesion in every case, a new name of “Focal Scleral Nodule” is proposed.

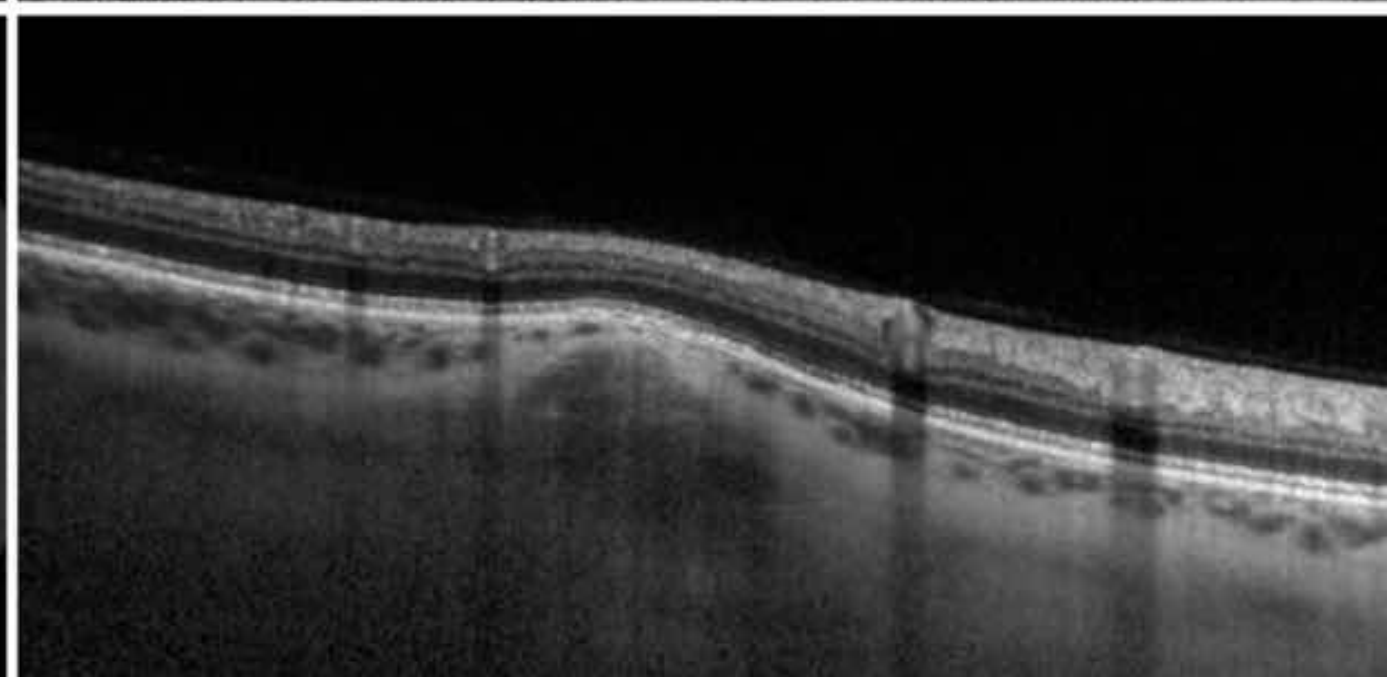
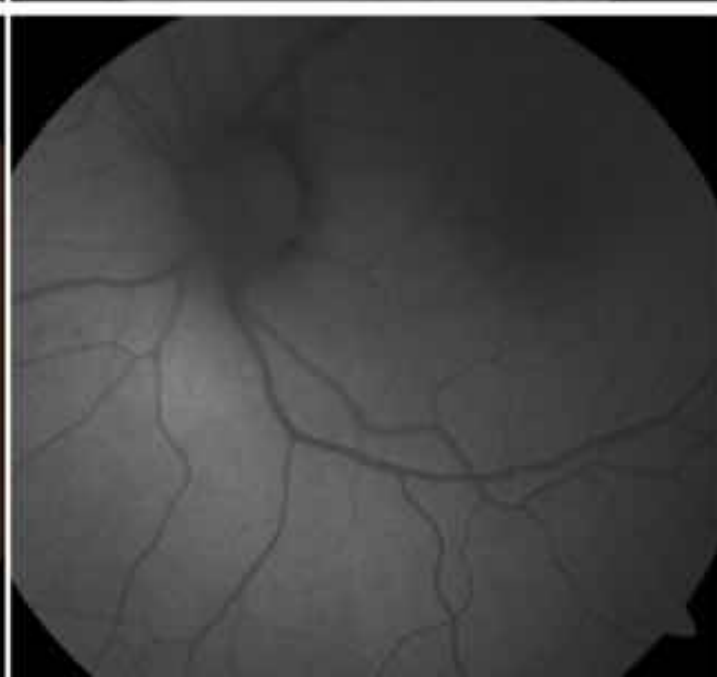
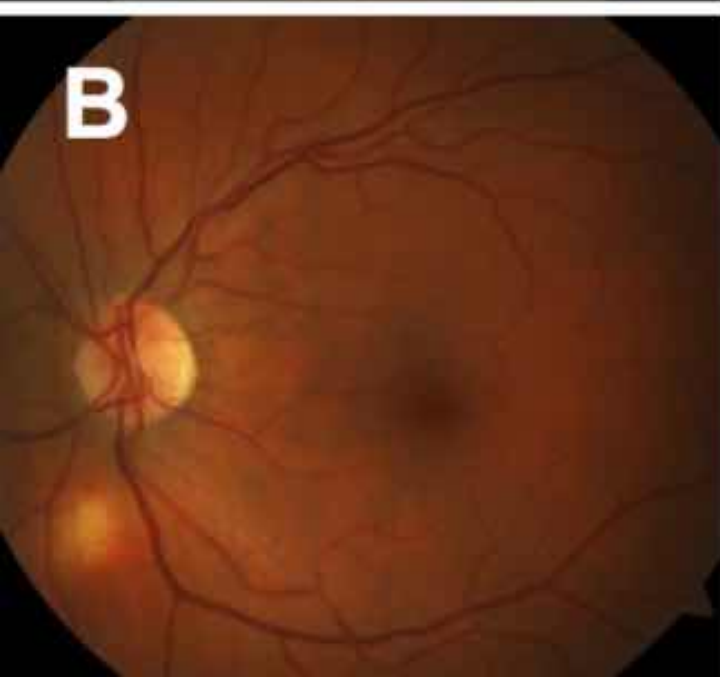
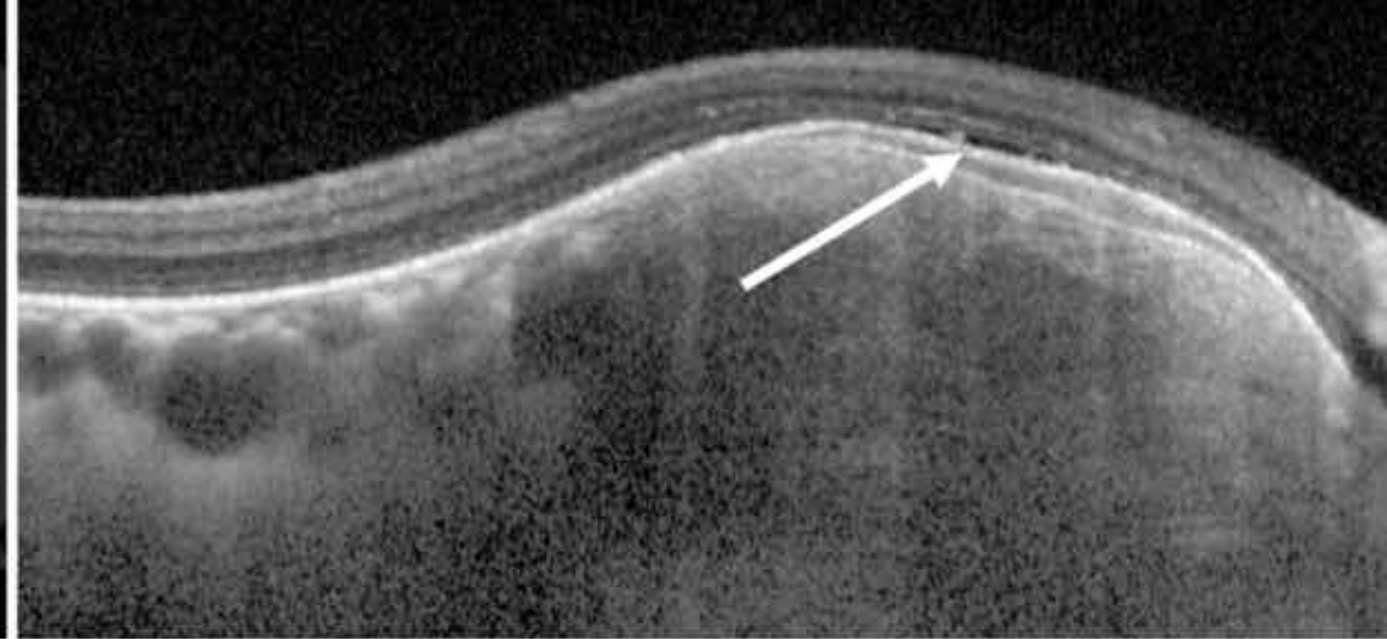
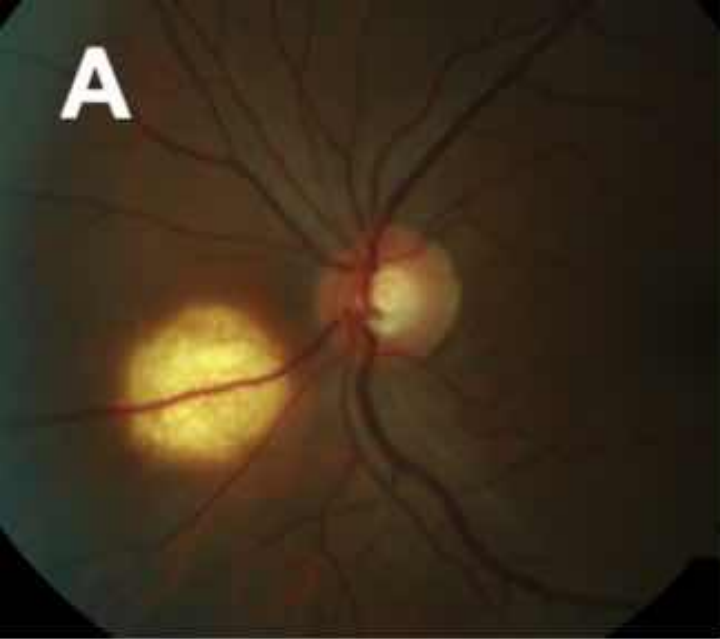
In 1997 Hong et al.<sup>1</sup> reported six cases of a previously undescribed clinical entity that they named “Unifocal Helioid Choroiditis”, because of its sun-like appearance. These unilateral, unifocal, round, yellow-white lesions were approximately 1 disc-area in size and located near the optic nerve. In 2002, Shields et al.<sup>2</sup> described 60 similar lesions, but termed the disorder “Solitary Idiopathic Choroiditis” (SIC), based on a focal, non-neoplastic choroidal elevated mass.<sup>3-7</sup> Both Hong et al.<sup>1</sup> and Shields et al.<sup>2</sup> described this lesion prior to the widespread availability of optical coherence tomography (OCT) and attributed the yellow-white lesion to choroidal inflammation. Shields et al.<sup>2</sup> observed that this lesion displayed features similar to choroidal granuloma but without systemic evidence of a secondary cause including tuberculosis, sarcoidosis and toxocariasis. Furthermore, in these 2 series, some patients described symptoms (not necessarily associated) and a minority exhibited “uveitis”, “vitritis” or “subretinal fluid”. Fluorescein angiographic leakage or staining was evident in some eyes.<sup>1,2</sup>

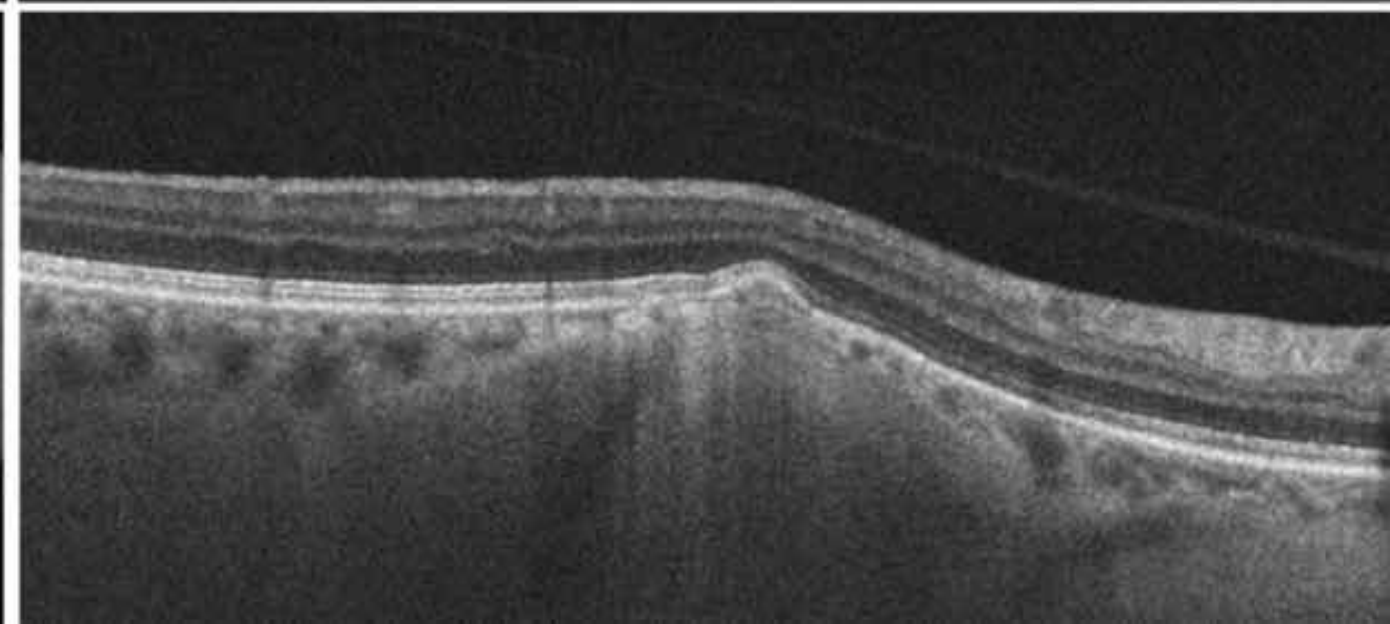
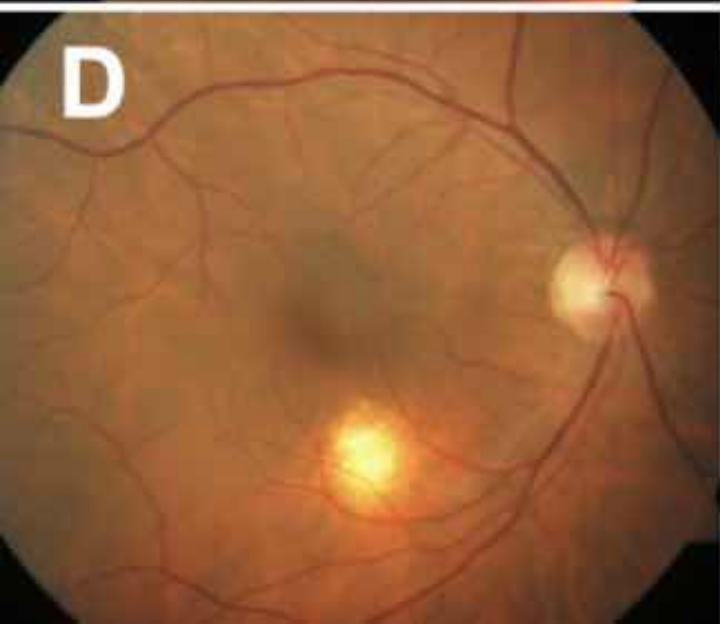
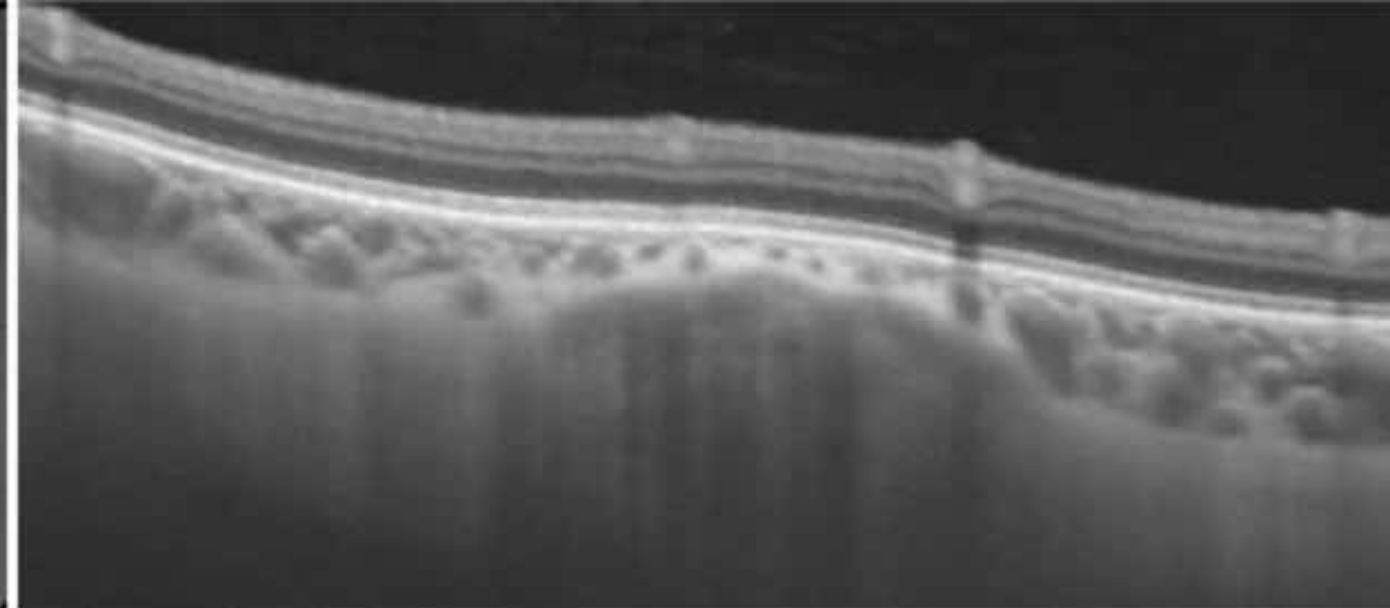
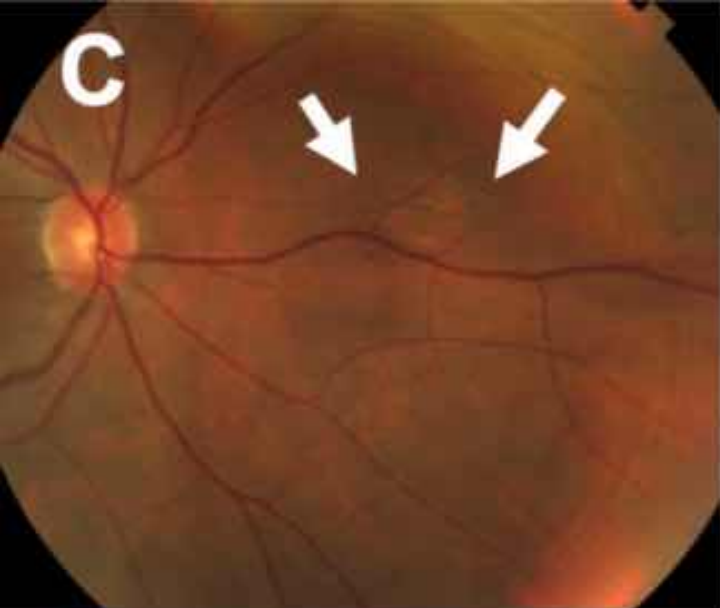
### *Definition of Solitary Idiopathic Choroiditis*

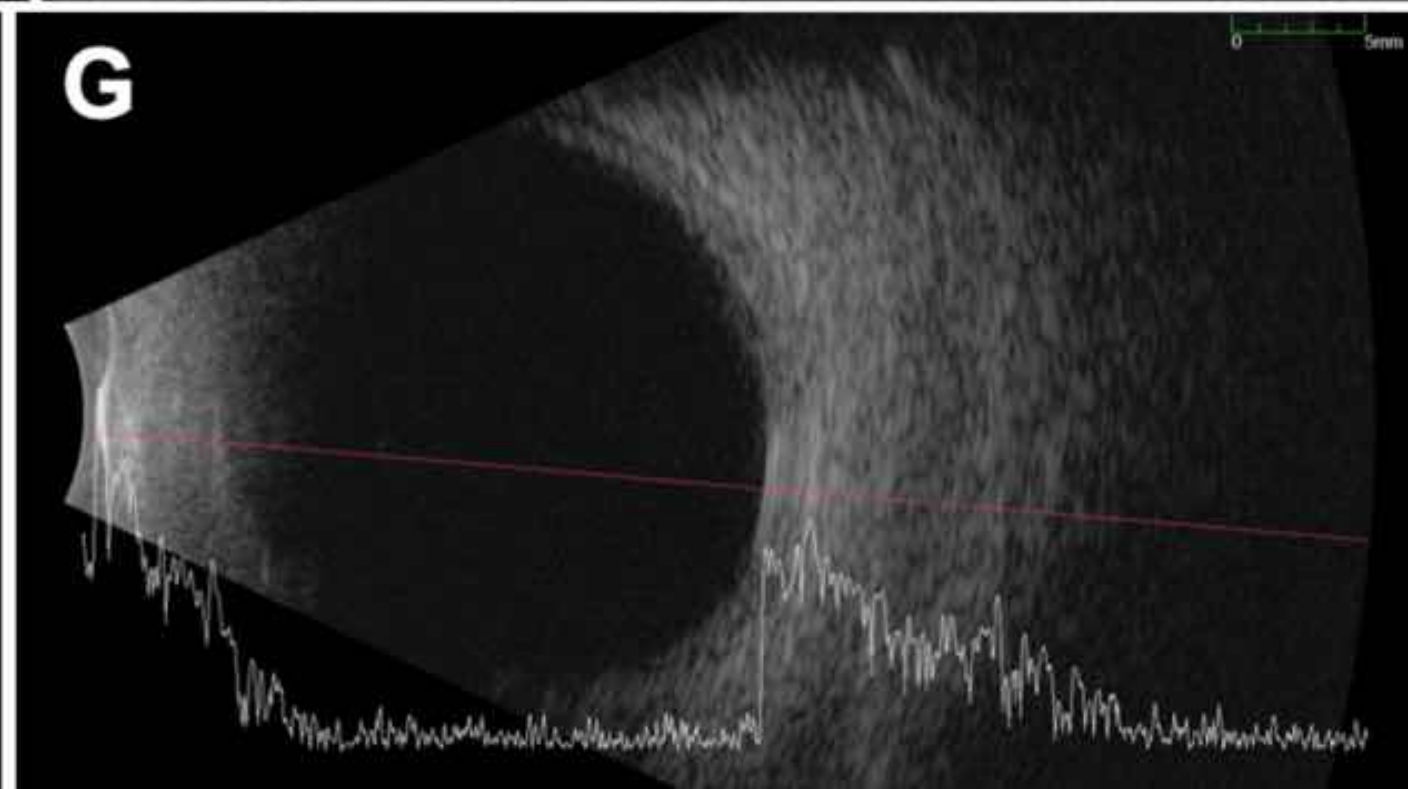
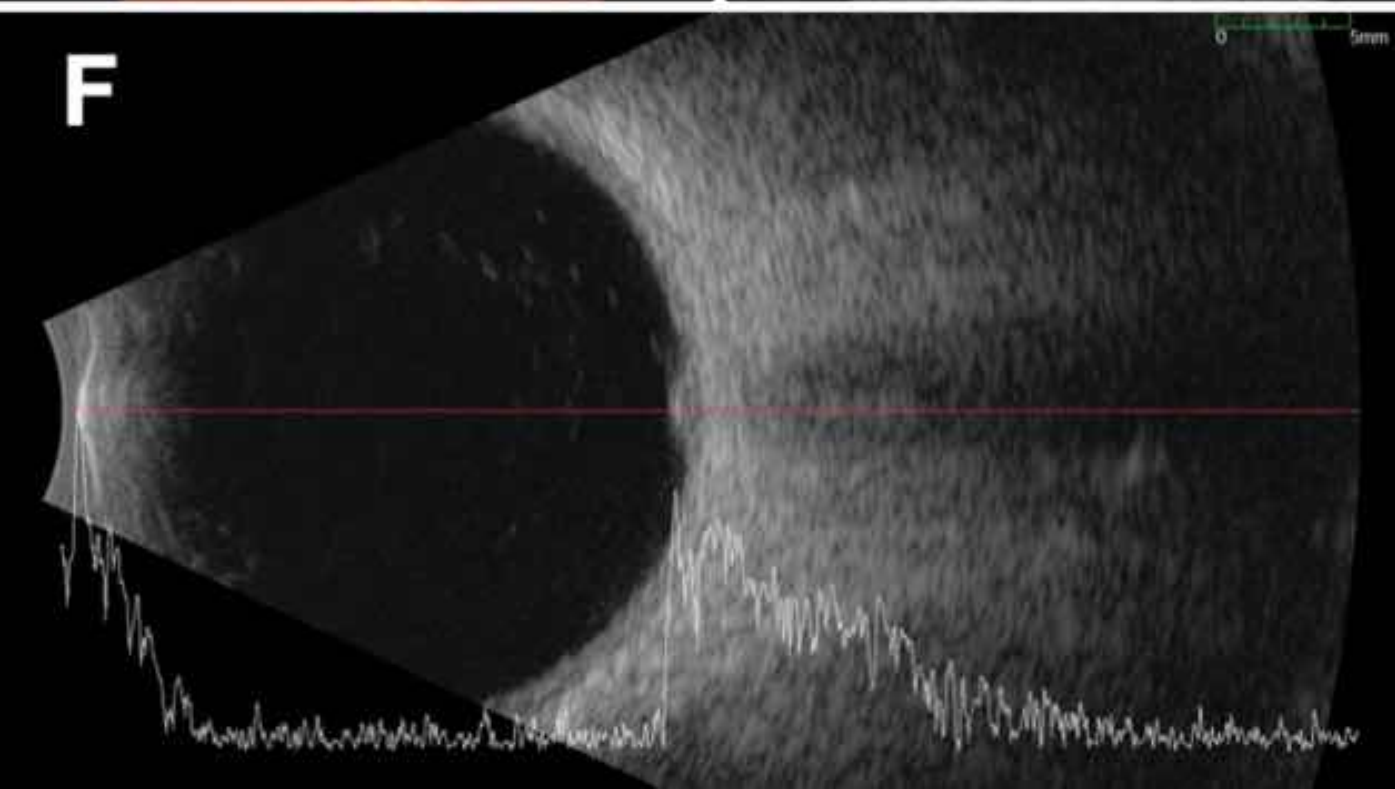
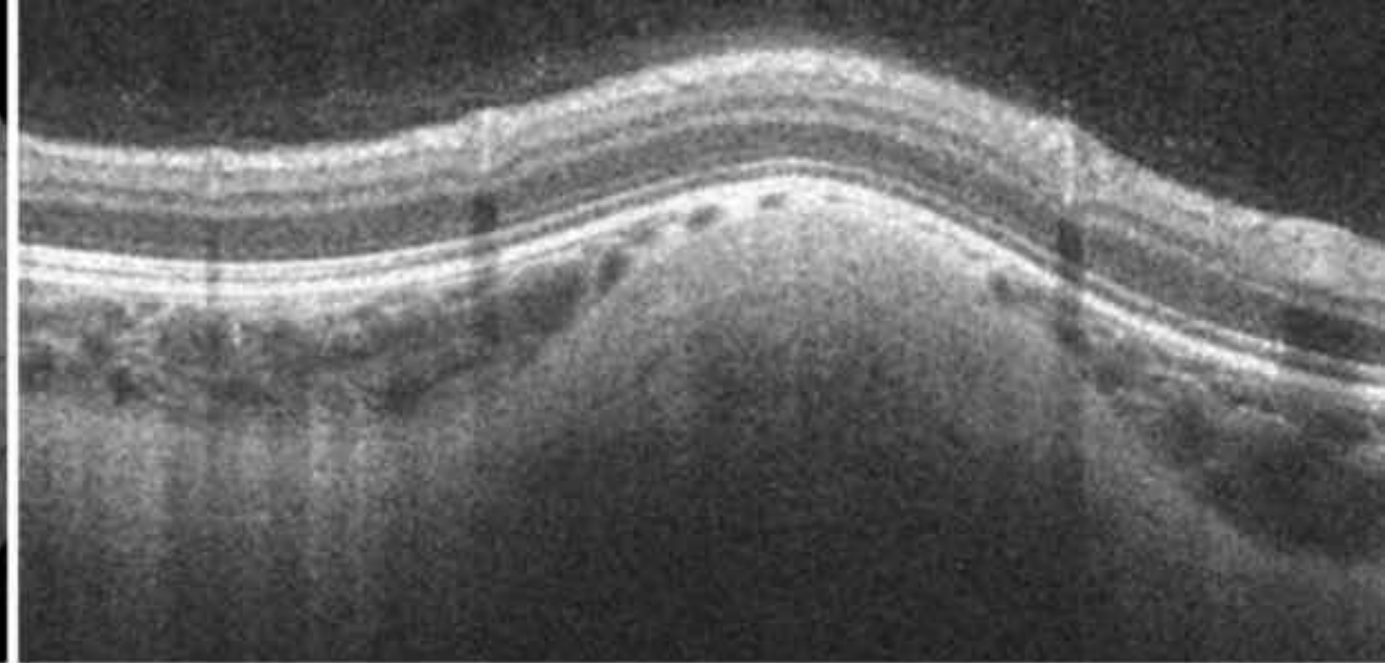
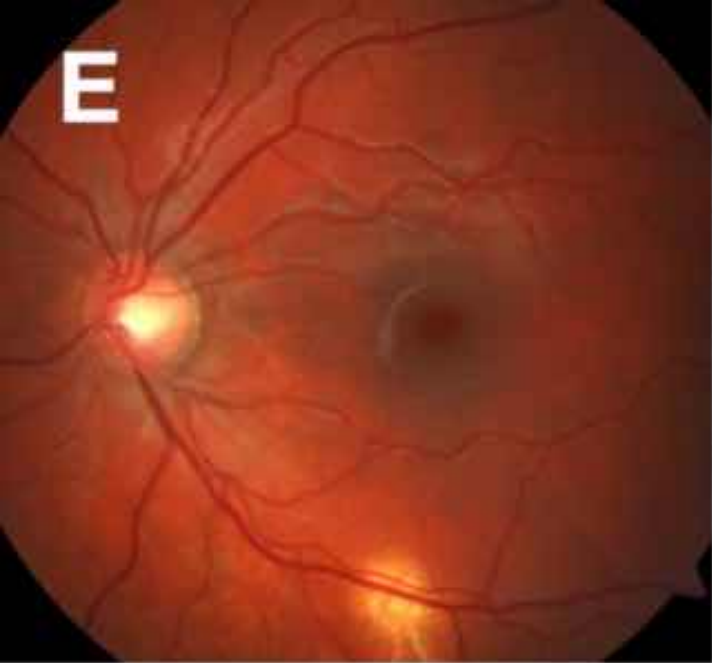
Based on the seminal paper by Shields et al.<sup>2</sup>, SIC was defined as a circular yellow-white subretinal fundus lesion without associated systemic disease upon investigation. Based on multimodal imaging findings, similar looking fundus lesions in the choroid (amelanotic nevus, amelanotic melanoma, metastasis, osteoma, granuloma) or retina (retinoblastoma, astrocytic hamartoma), were excluded. The characteristic multimodal imaging findings of SIC are shown in **Figure 1**.

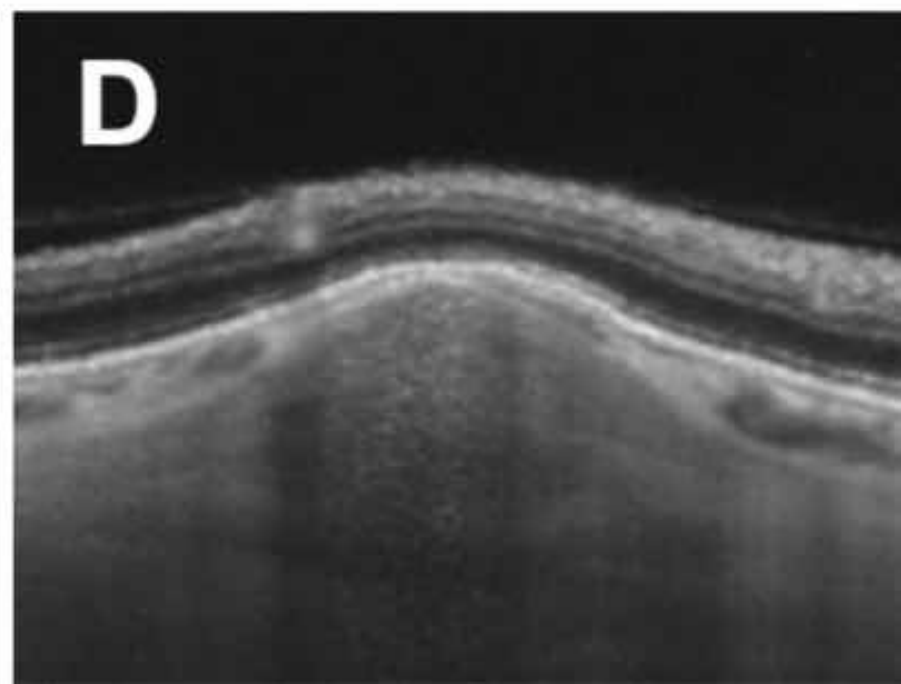
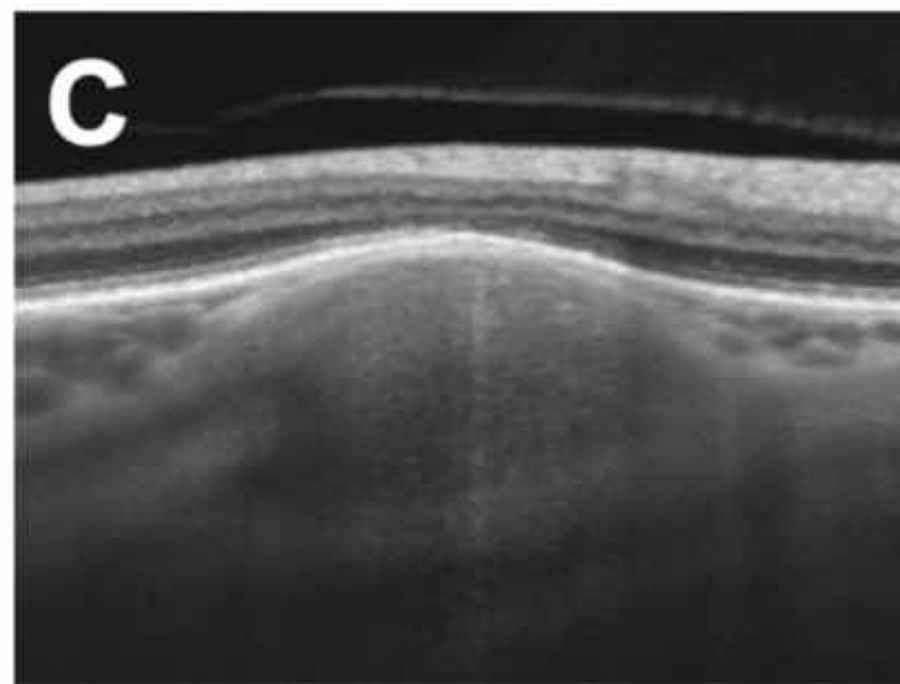
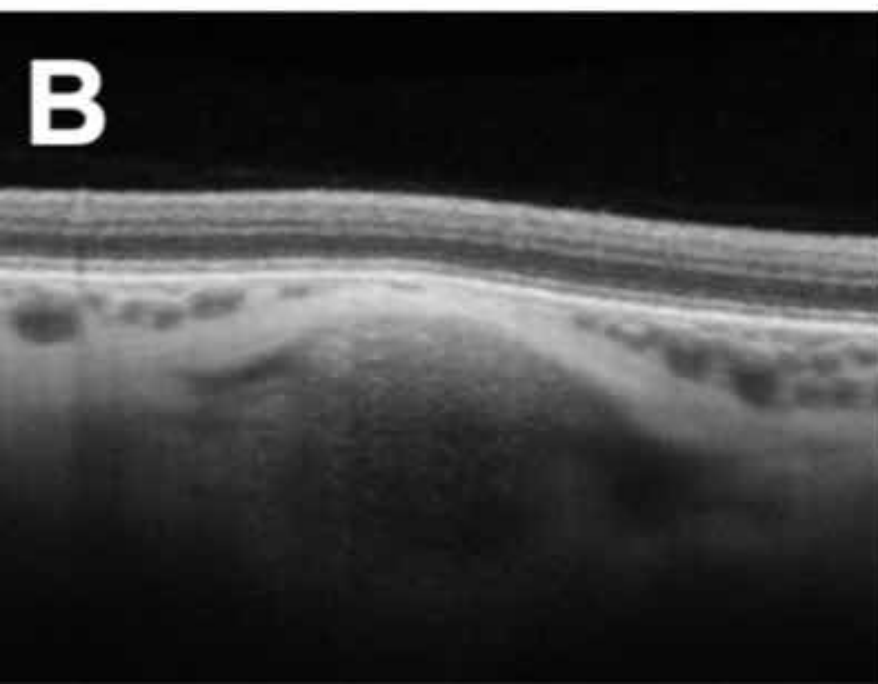
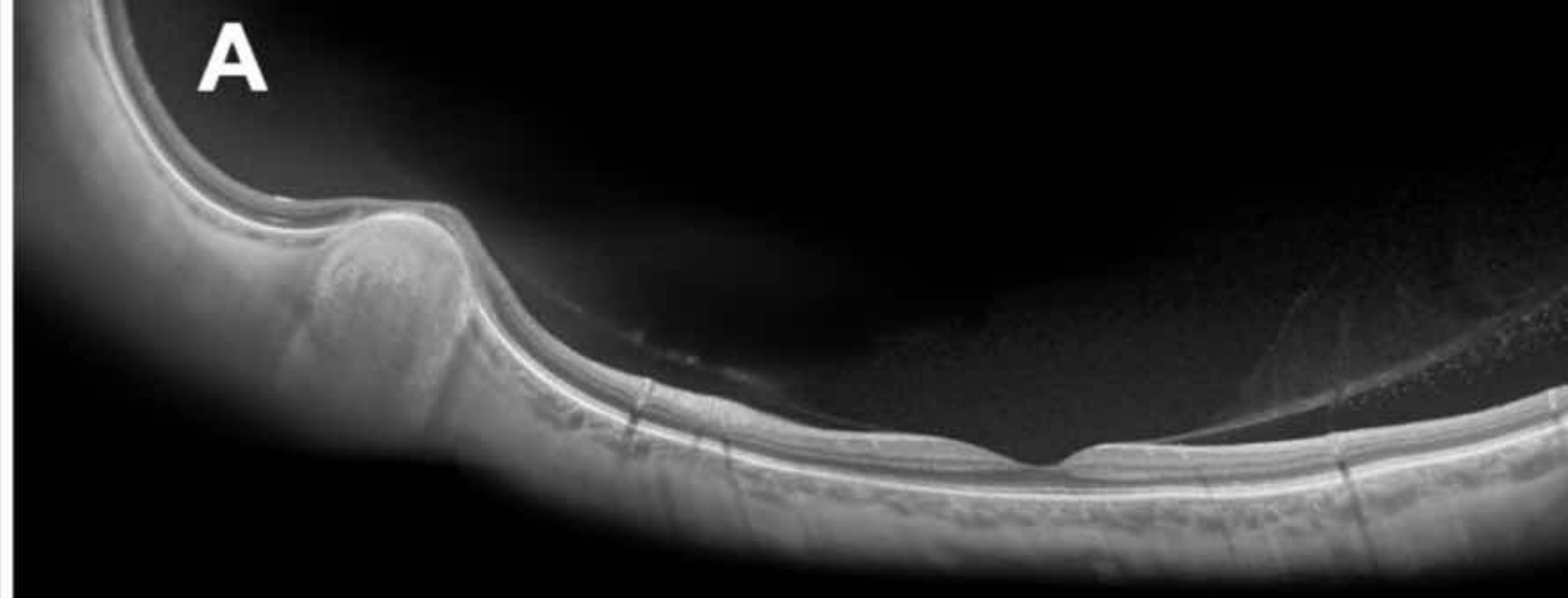
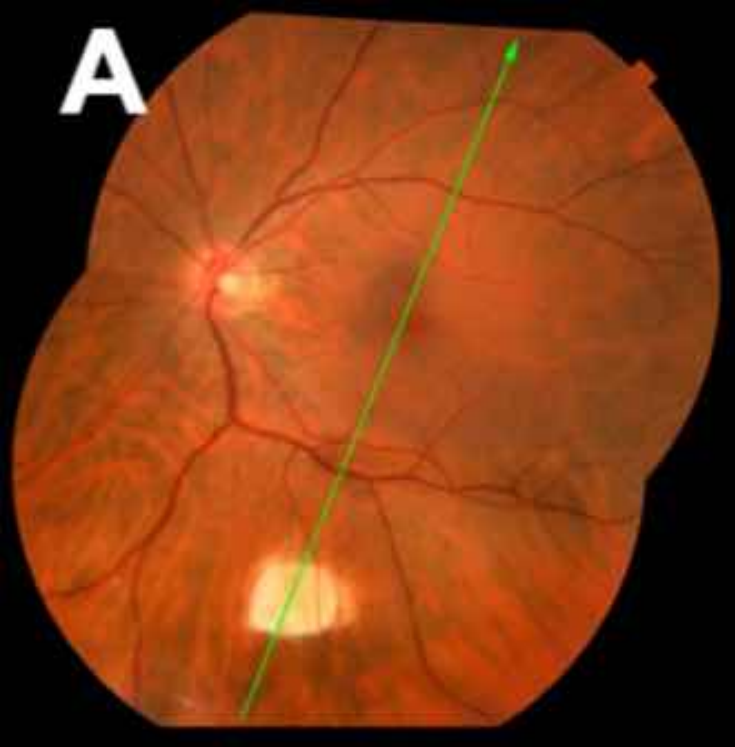
## *Clinical features*

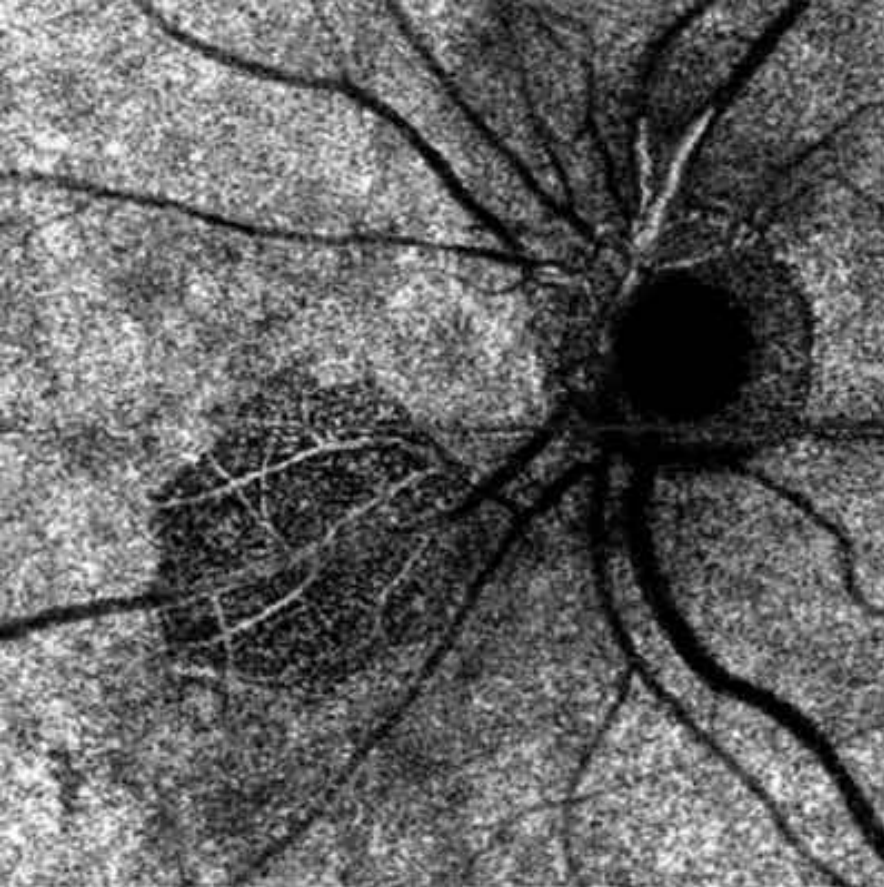
The clinical features of SIC lesions are summarized in **Table 3**. All lesions showed clearly demarcated borders and none exhibited signs of active inflammation, blurry margins, hemorrhage or exudation. On average, the lesions measured 1 disc area in size (mean basal diameter 2.4 x 2.1 mm) and were typically yellow in color (54%), without associated drusen (98%) or orange pigment (97%). An orange halo was present in 44% of cases. Example images of the halo are provided in **Figure 1**. Thirty-three percent of lesions displayed overlying or surrounding RPE changes including hypopigmentation (n=18) and hyperpigmentation (n=3). The lesions were typically found in the peripapillary area, inferonasal to the disc, with a mean distance of 2.4 mm (median 2.2, range 0-6.8mm) from the optic nerve. All lesions were located post-equatorial and the majority of lesions (64%) were located in the inferior hemisphere. Only four (7%) lesions were identified at the macula and the mean distance to the fovea was 4.4 mm (median 4.2, range 0.5-11.9 mm). None of the eyes showed signs of vitritis. The spectrum of these findings is illustrated in **Figure 1**.



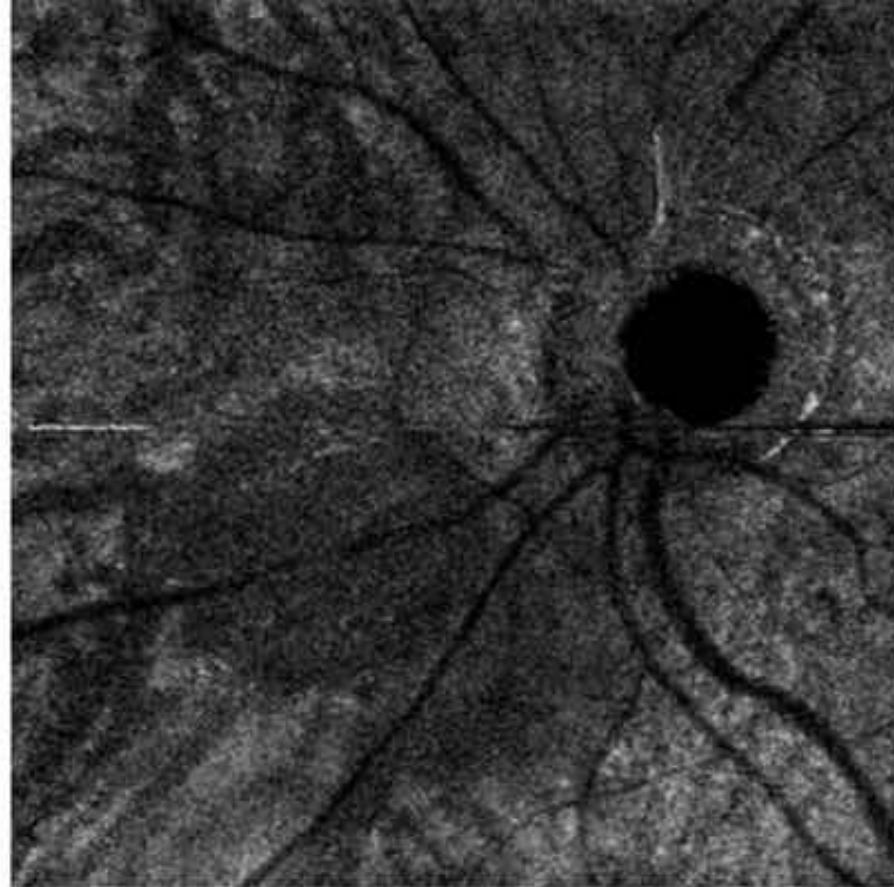




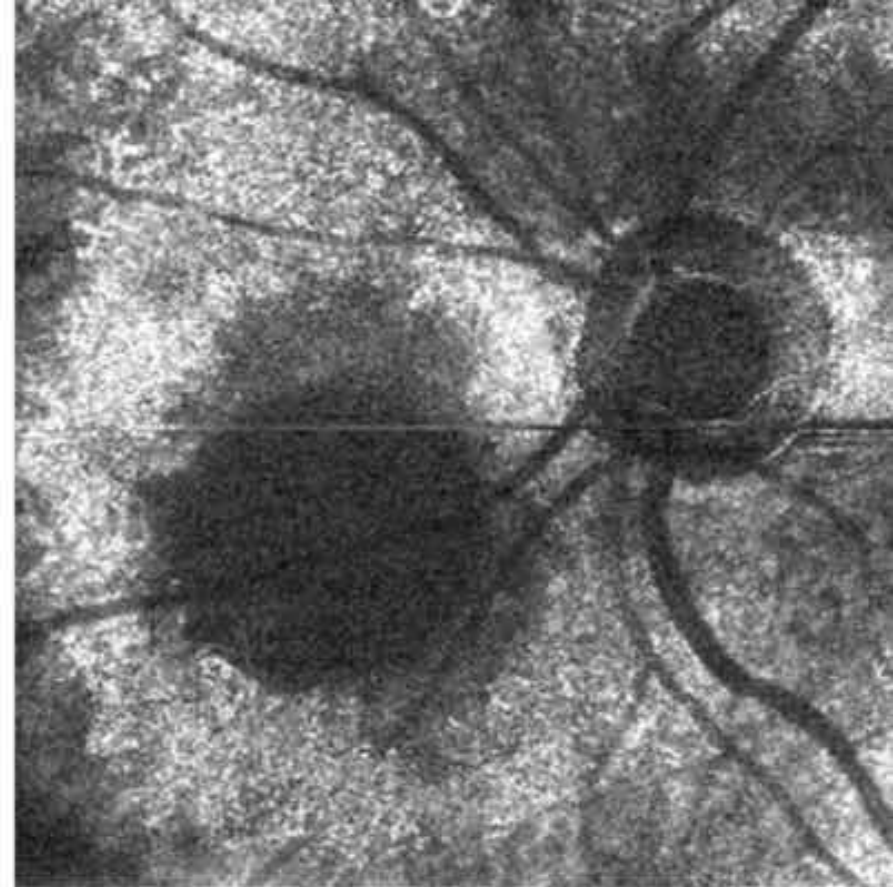
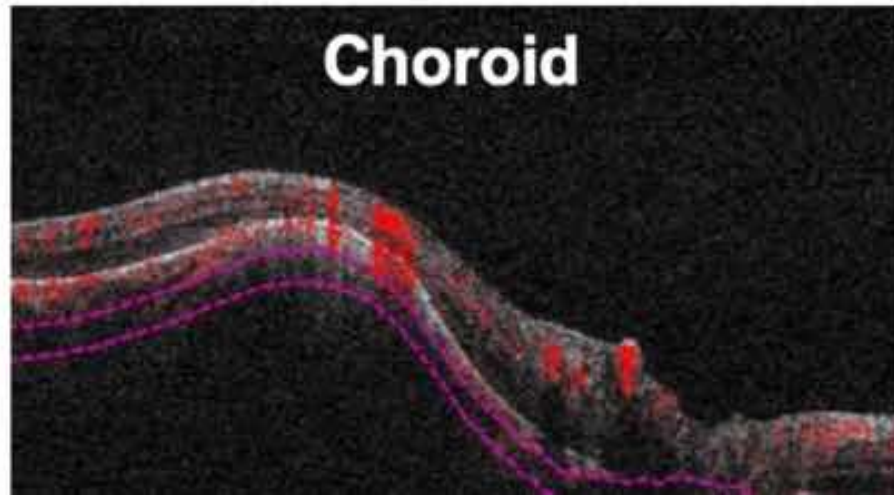




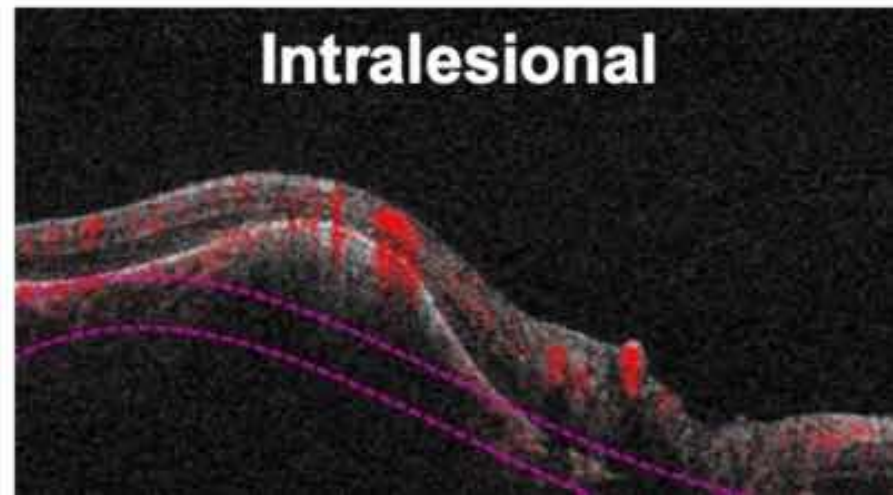
**Choriocapillaris**



**Choroid**



**Intralesional**



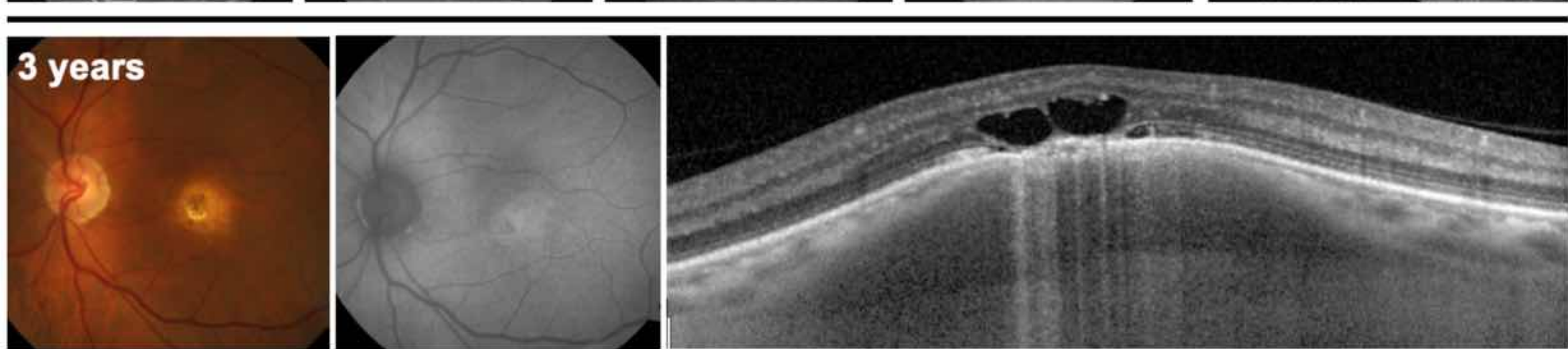
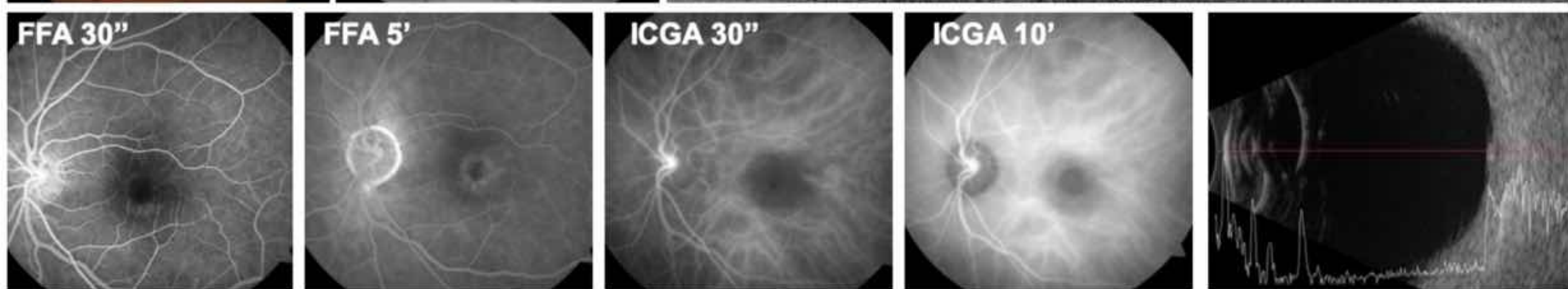
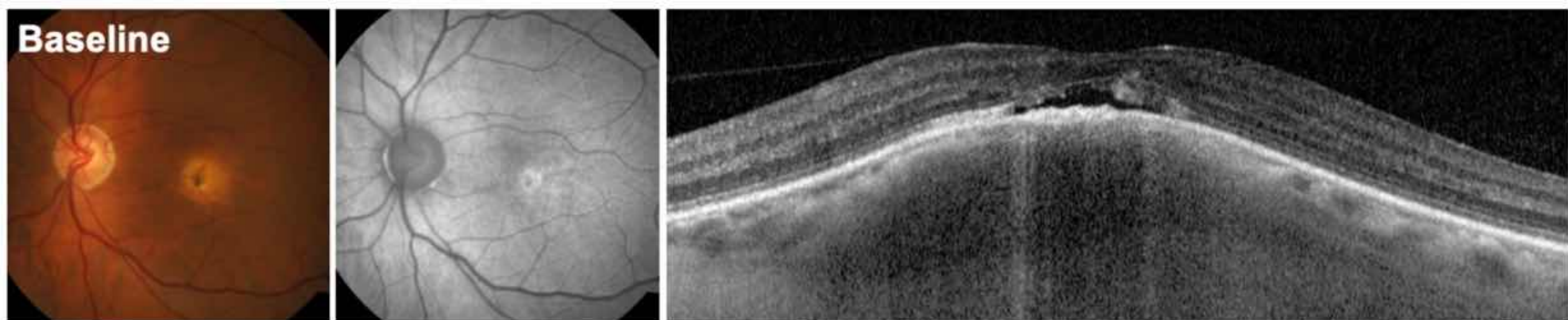


**Figure 4:** Solitary idiopathic choroiditis (SIC) lesion at the fovea. This 53-year-old man presented with a reduced visual acuity of 20/80. A yellow, lesion measuring 2.3 mm x 2.3 mm with pigmentary mottling showing hyperautofluorescence was present at the macula. Enhanced depth imaging optical coherence tomography demonstrated a typical intrascleral, dome-shaped lesion with loss of overlying choroidal vasculature and retinal pigment epithelium irregularity. This eye also showed a cleft of subretinal fluid with subtle accumulation of pseudovitelliform material. Fundus fluorescein angiography (FFA) demonstrated late-phase staining but on indocyanine green angiography (ICGA) the lesion remained hypofluorescent. B-scan ultrasonography demonstrated a hyperechogenic lesion without extra-ocular extension or shadowing that would suggest calcification.

After three years of follow up (bottom row), the SIC lesion remained stable in dimensions, although

progressive retinal pigment epithelial atrophy and degenerative cystoid intraretinal fluid had developed.

Visual acuity had deteriorated to 20/125.

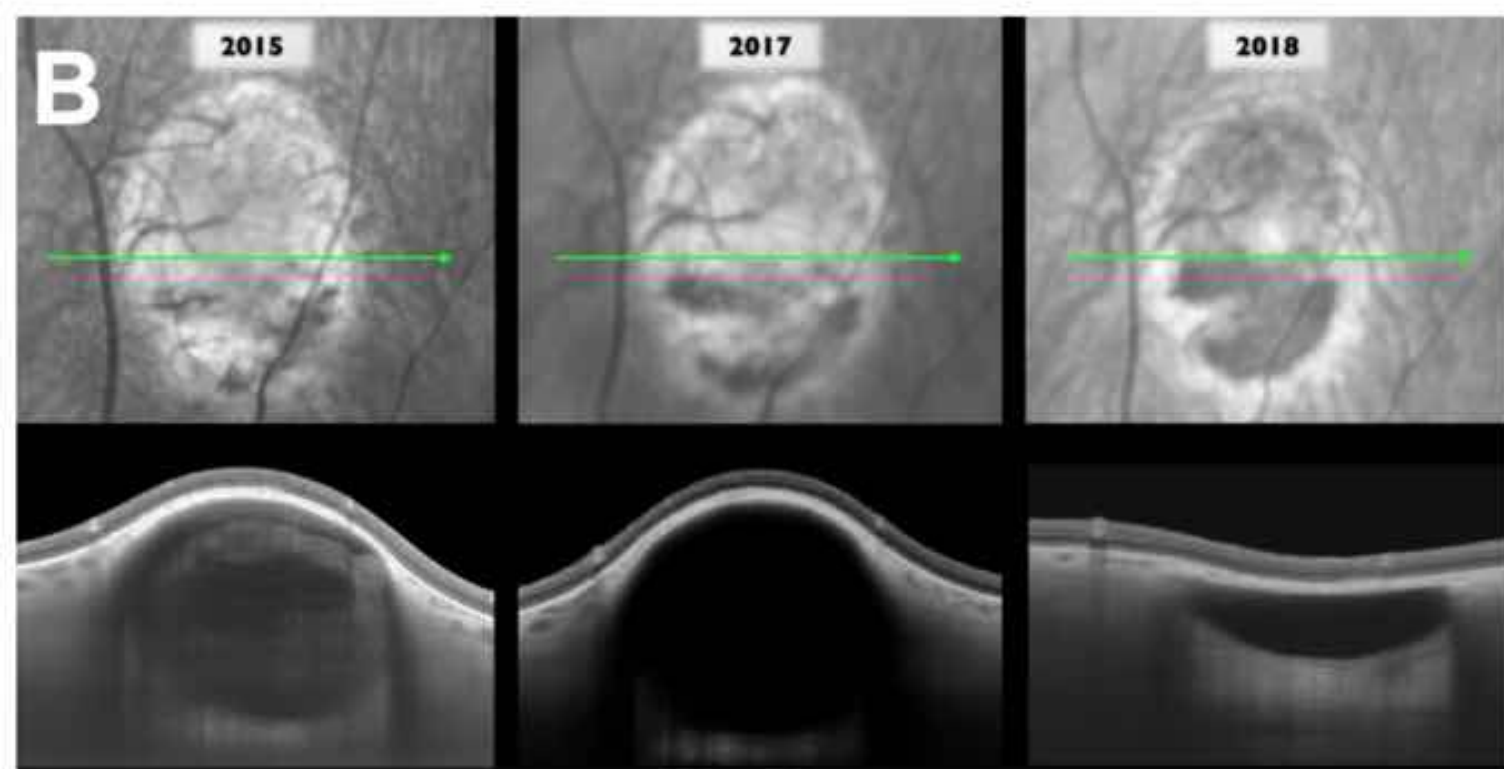
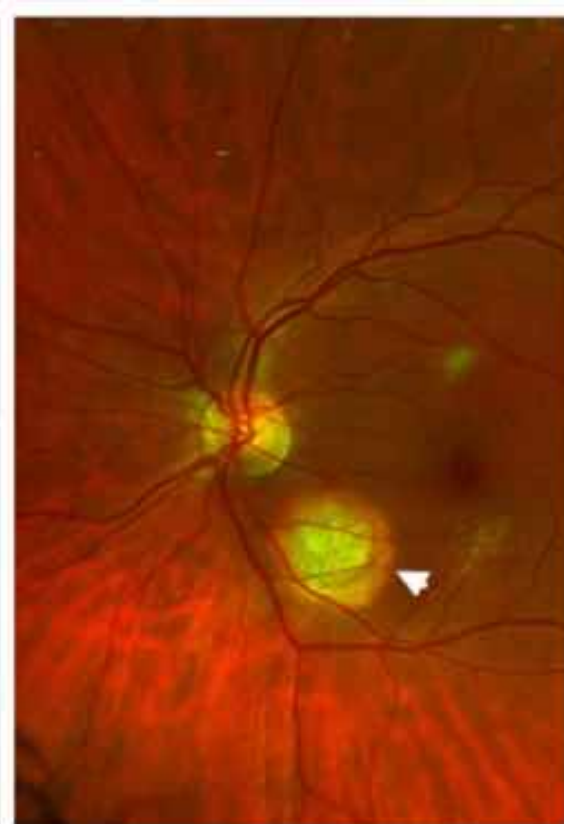
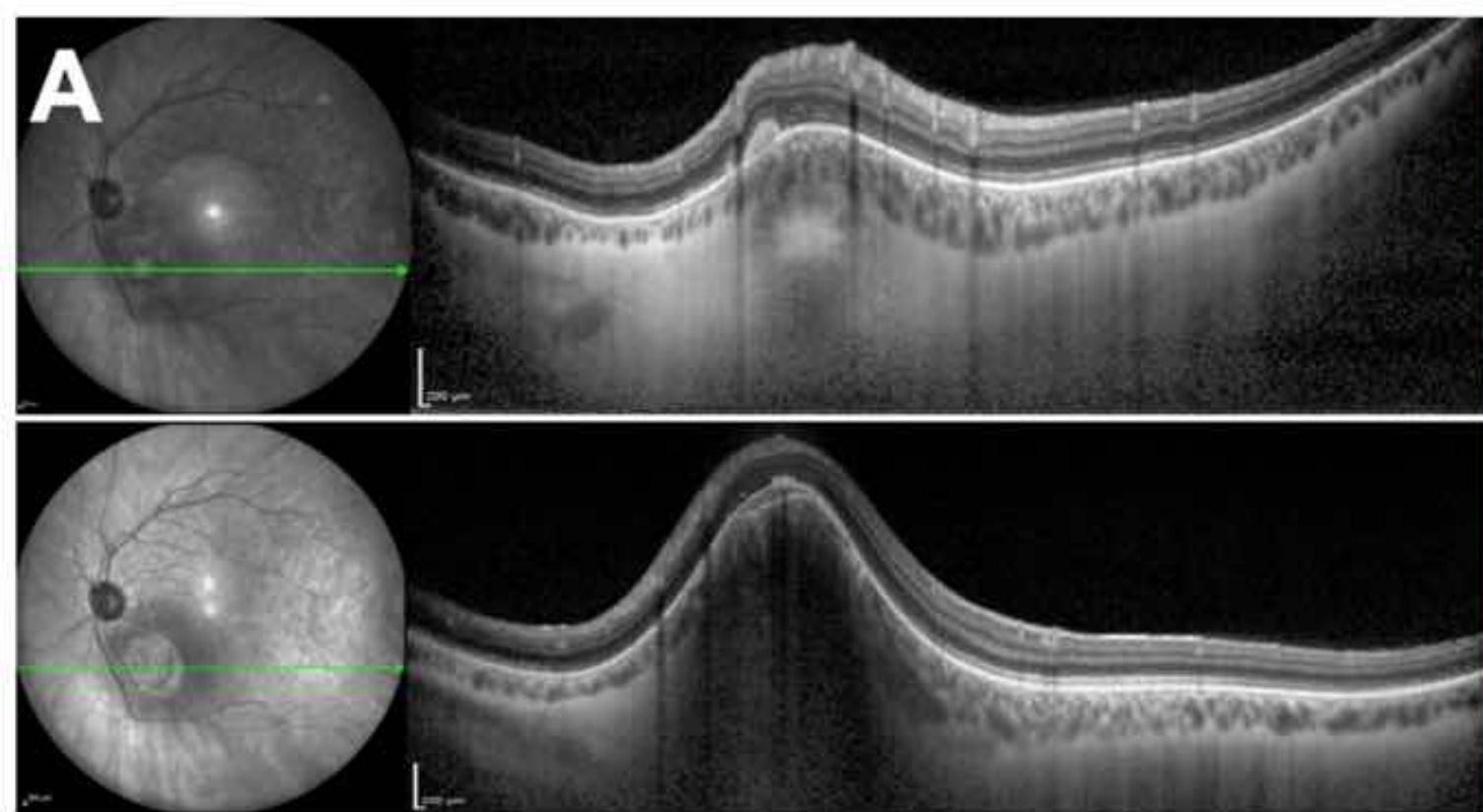


**Figure 5:** Changes in solitary idiopathic choroiditis (SIC) lesions over time.

One patient in our series (**A**) demonstrated a small intrascleral lesion with a hyper-reflective center and hypo-reflective mantle (top row of top panel). Five years later, a hypo-reflective domed-shaped scleral protrusion on optical coherence tomography consistent with SIC had developed (bottom row of top panel, pseudo-color photograph).

Another patient (**B**) experienced spontaneous regression of SIC. The first examination in 2015 showed the typical nodular configuration of the lesion in the sclera, with a visible posterior margin on swept-source optical coherence tomography imaging and diffuse hyperreflectivity. Two years later, the lesion became hyporeflective perhaps as a result of internal liquefaction. One year later the hyporeflective lesion had further regressed and focal choroidal excavation was noted. The near infrared images (top panel, bottom row) show changes in the reflectance of the lesion with topographic collection of hyporeflective material at the bottom of the lesion and formation of a pseudohypopyon-like appearance at the latest follow-up.

**Table 2: Focal scleral nodule in 63 eyes of 63 patients:  
Referral diagnosis.**

<b>Referral Diagnosis</b>	<b>No (%) of Patients</b>
Choroid Nevus, amelanotic	5 (8%)
Choroid Melanoma	5 (8%)
Sclerochoroidal Calcification	4 (6%)
Choroid Osteoma	4 (6%)
Choroid Granuloma	3 (5%)
Choroid Metastasis	2 (3%)
Solitary Idiopathic Choroiditis	2 (3%)
Choroiditis, unspecified	1 (2%)
Choroid Lymphoma	1 (2%)
Choroid Scar	1 (2%)
Choroid Freckle	1 (2%)
Choroid / Retina lesion, unspecified	28 (44%)
No diagnosis	5 (8%)

---

**Location relative to optic nerve**

Inferior 13 (21%)

Superior 6 (10%)

**Inferonasal** 15 (24%)

Inferotemporal 12 (19%)

Superonasal 7 (11%)

Superotemporal 10 (16%)

---

**Post-equatorial location** 63 (100%)

**Table 4: Focal scleral nodule in 63 eyes of 63 patients: Multimodal Imaging Findings.**

---

**Optical Coherence Tomography**

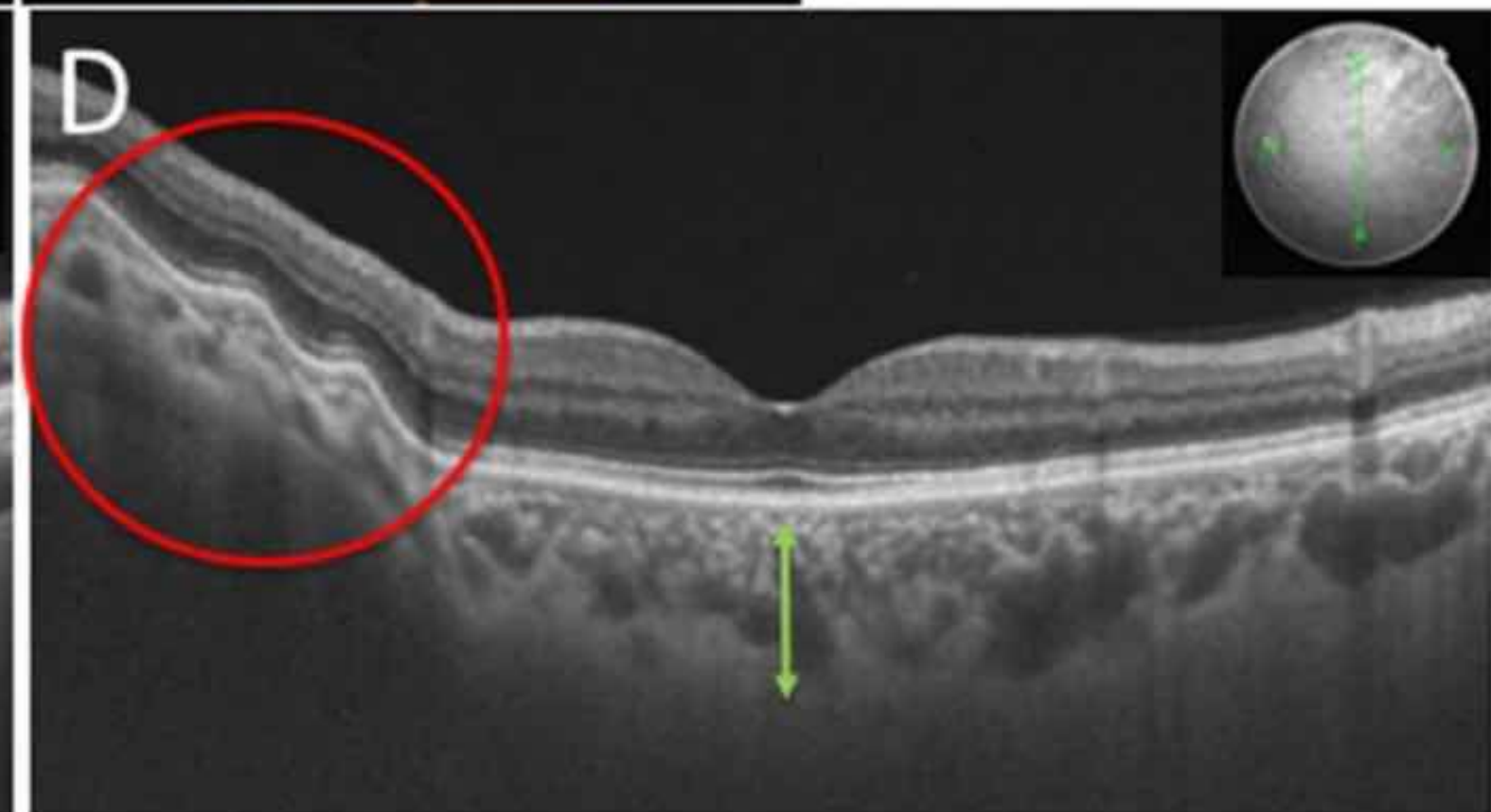
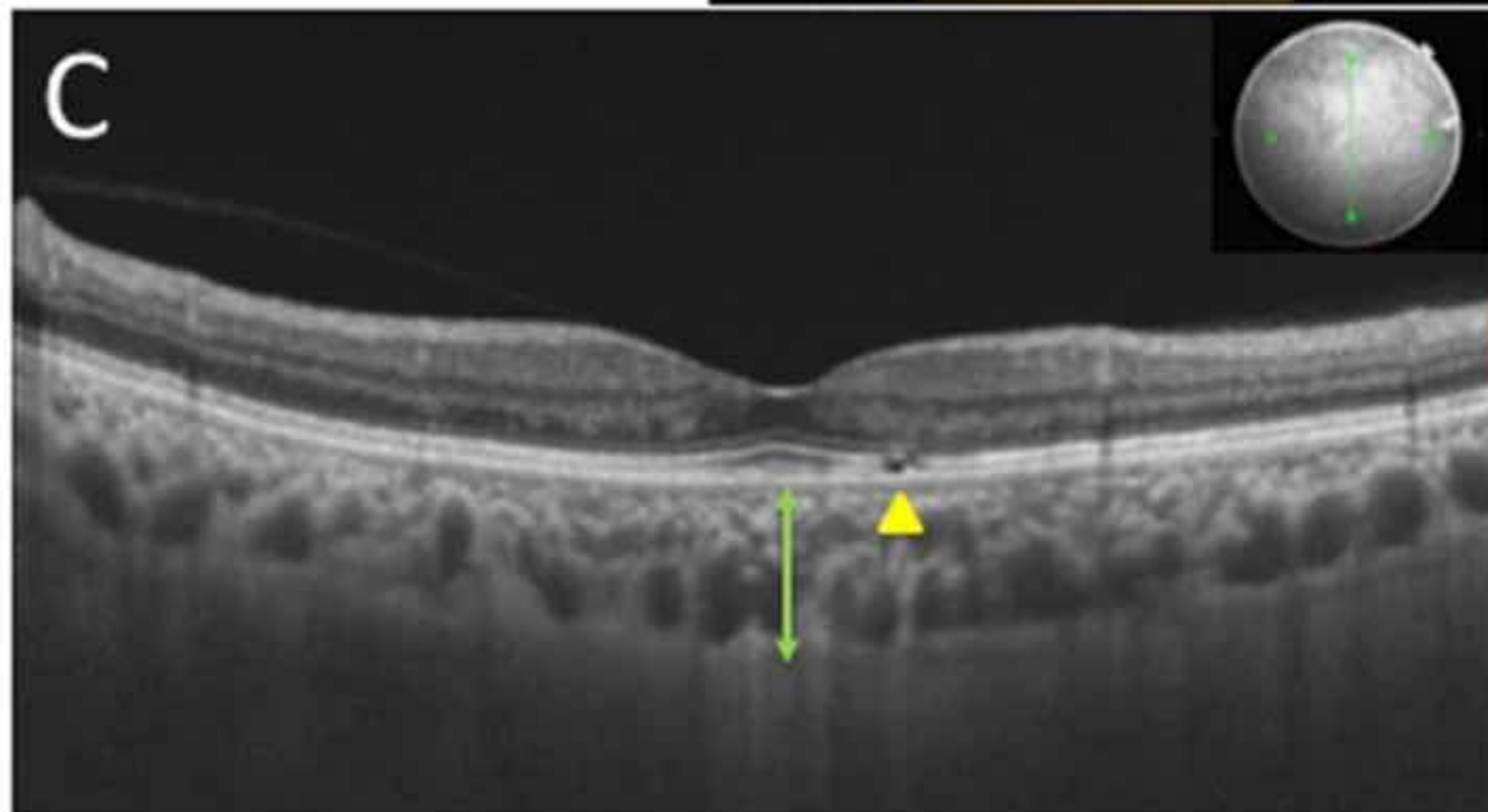
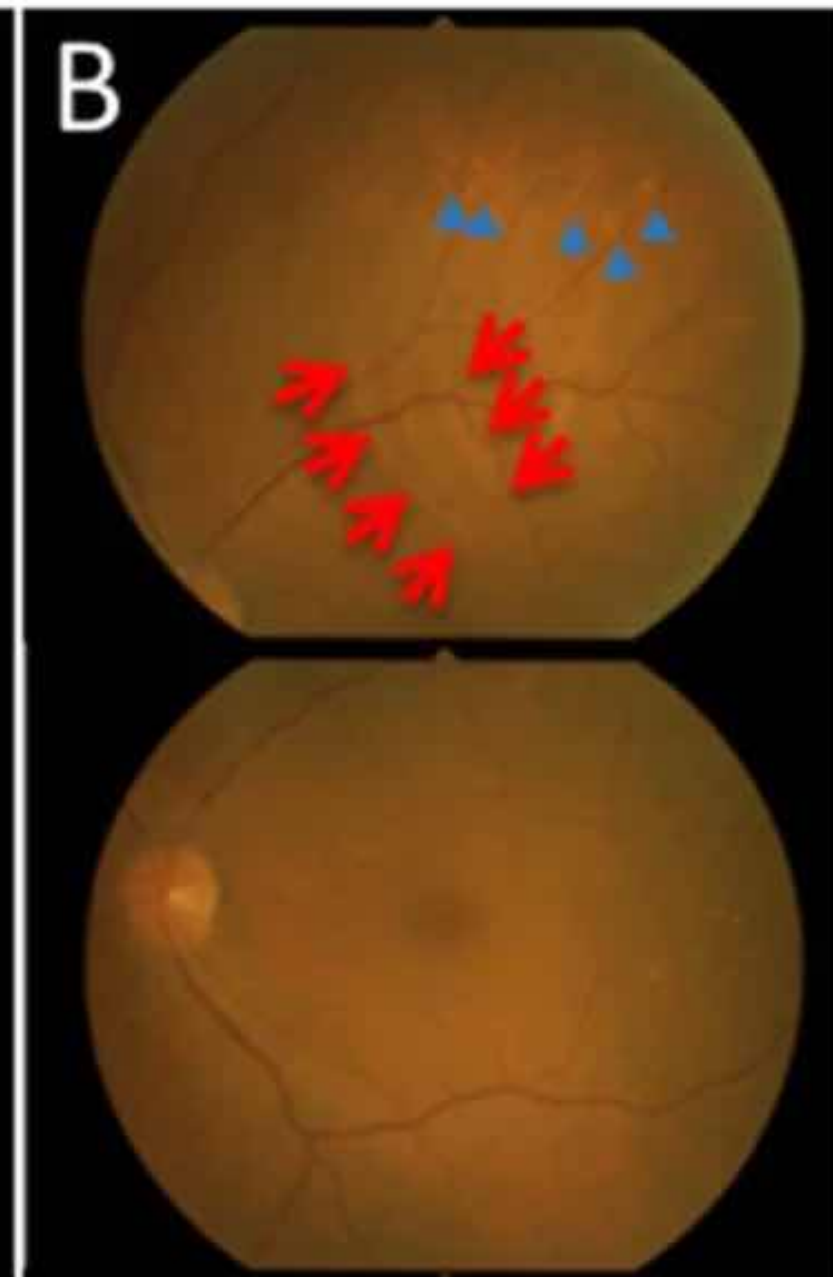
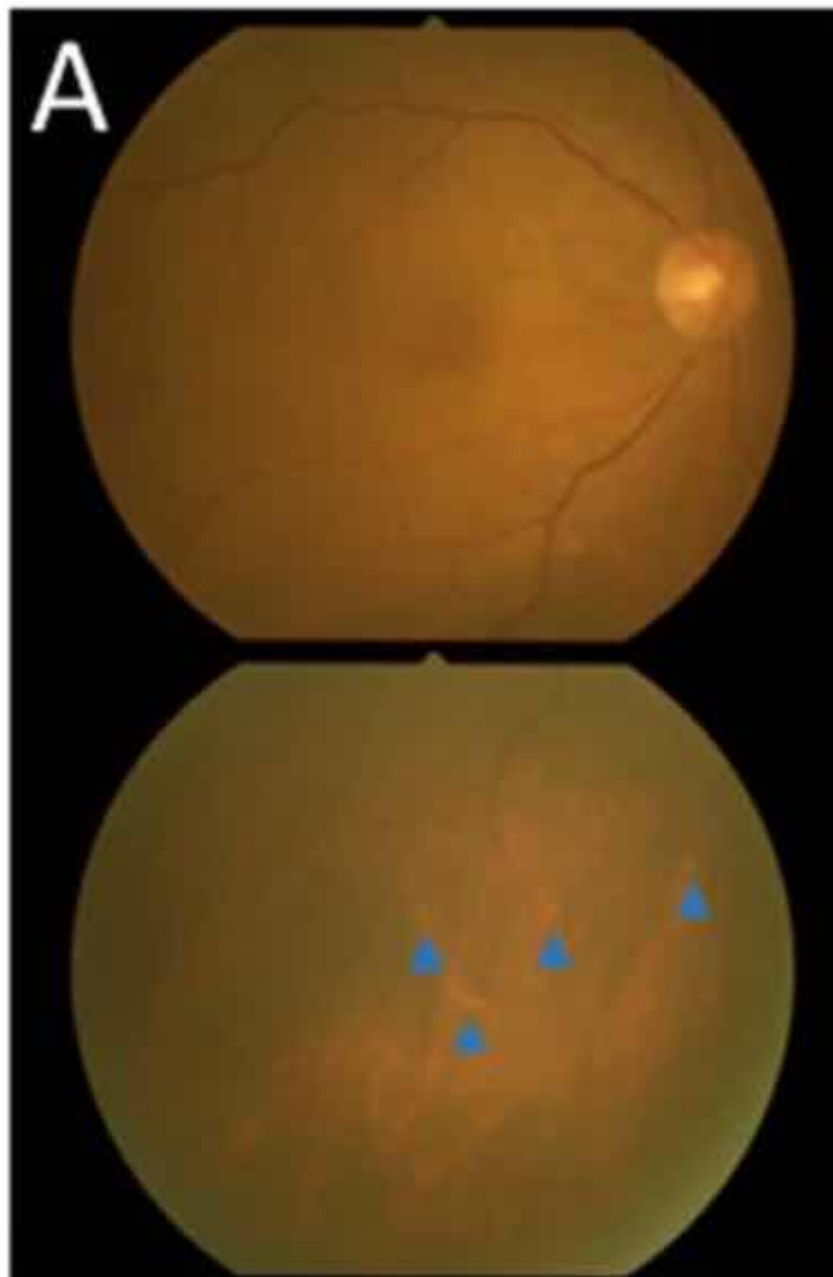
**Mean Horizontal Length (mm)**                       $2.6 \pm 0.9$

**Mean Thickness (micron, n=12)**                       $583 \pm 98$

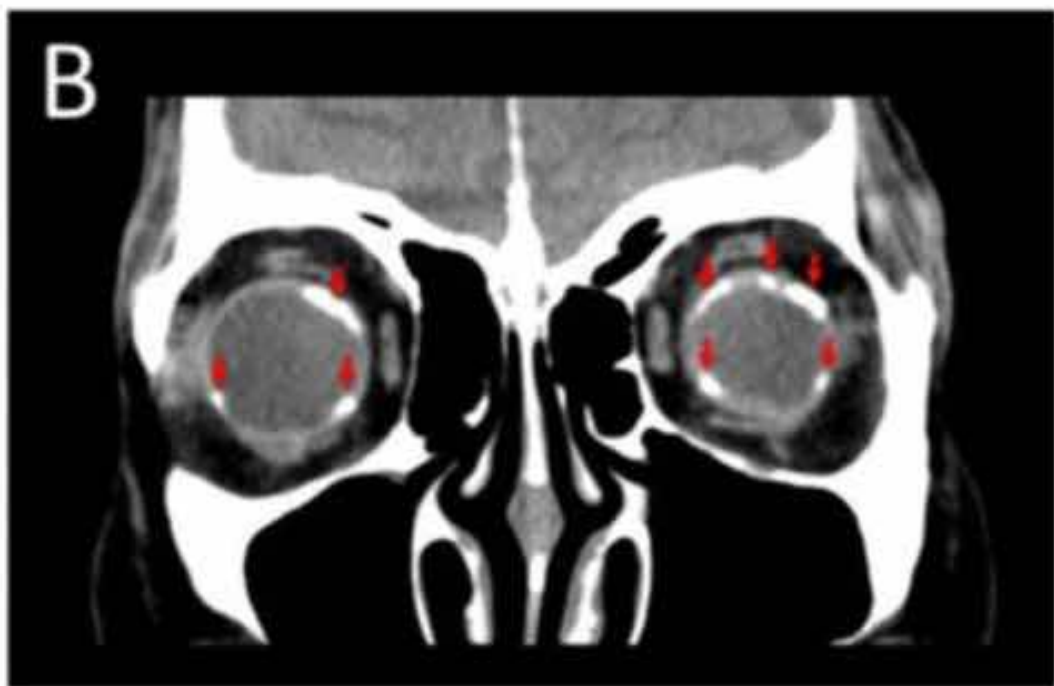
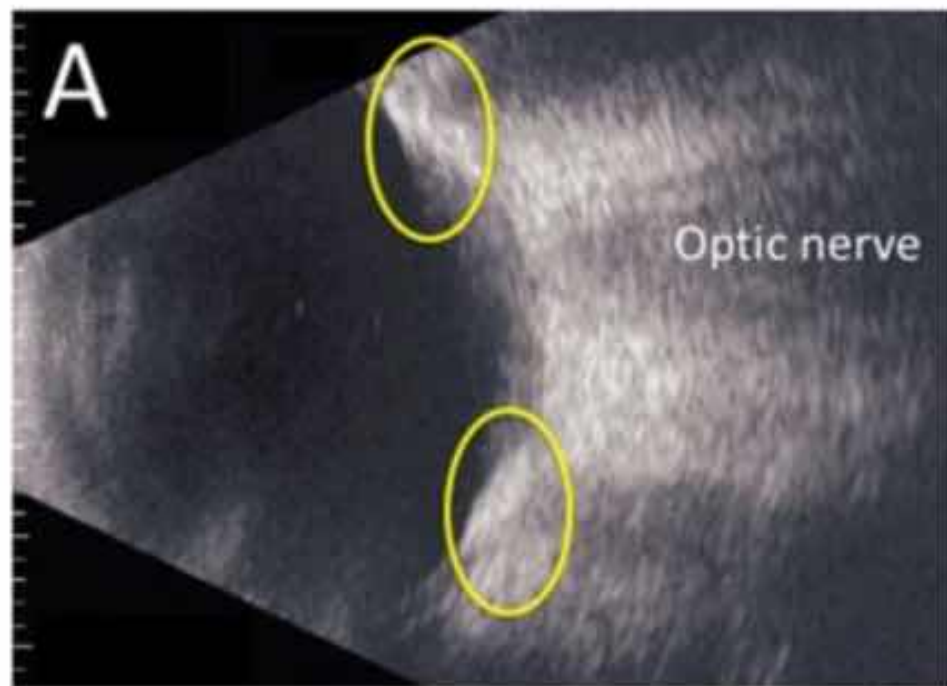
**Configuration**                      **Dome** 46 (73%)                      **Nodule** 12 (19%)                      **Volcanic** 5 (8%)

One condition that most closely resembles FSN is sclero(choroidal) calcification (SC).<sup>20</sup> In this disease, OCT imaging has shown that these lesions are primarily scleral as well, such that SC may be better named scleral calcification.<sup>21</sup> Thinning of the choroid overlying the areas of scleral thickening is

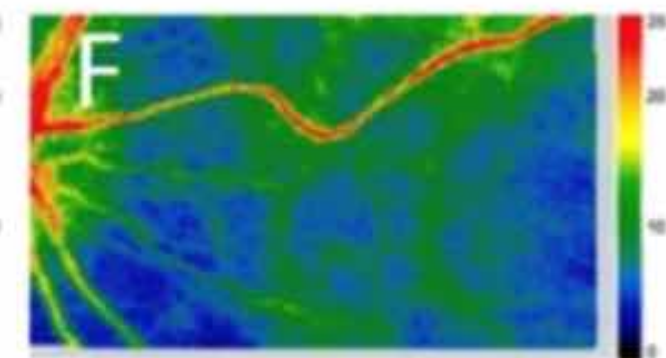
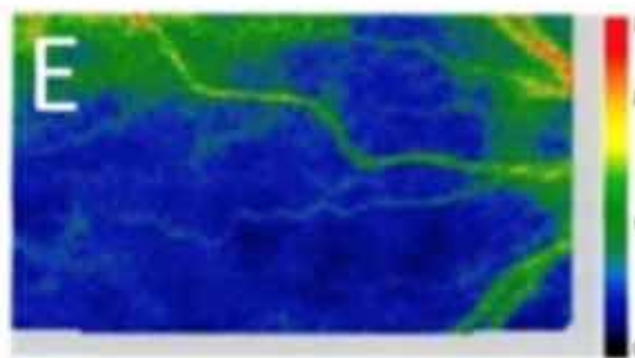
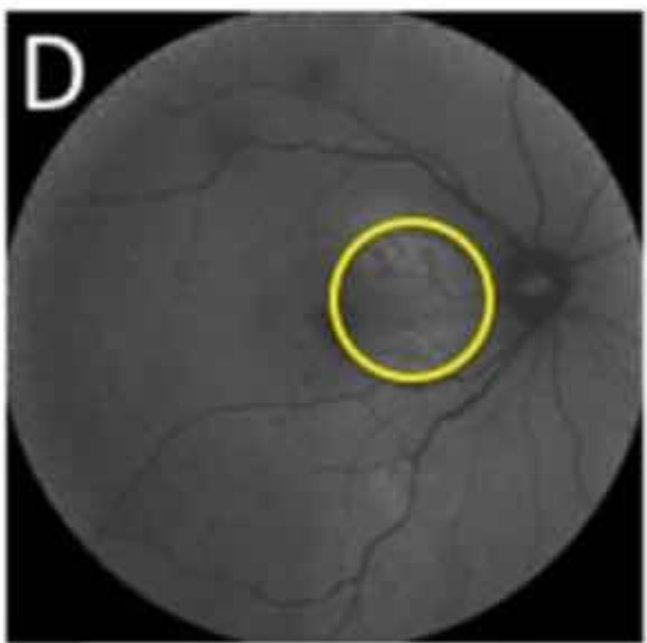
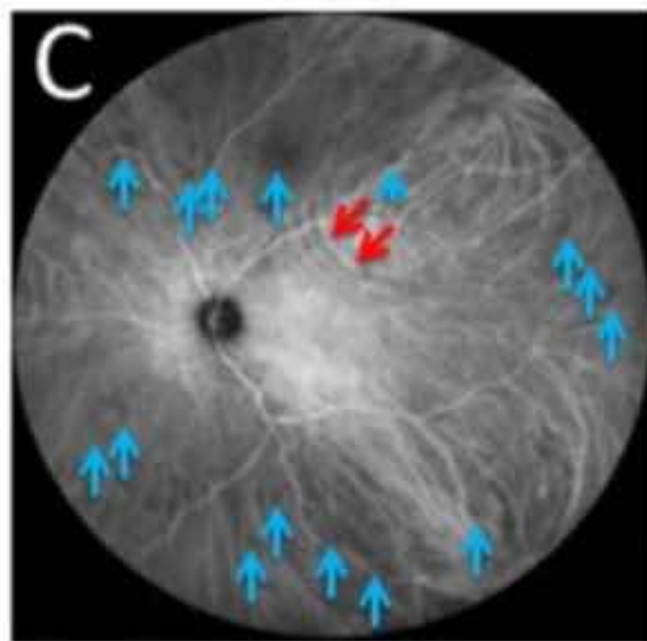
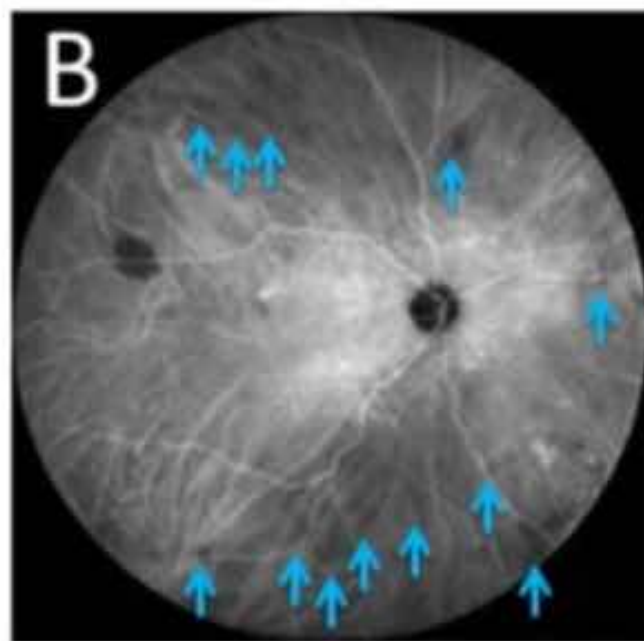
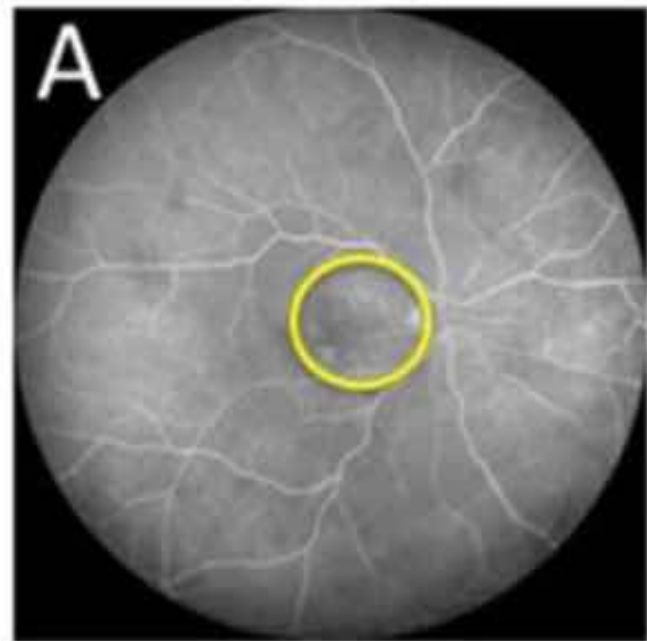
also seen. There are however a few features that can help differentiate FSN from SC. While FSN tends to be posterior and around the optic nerve, SC is usually more peripheral, anterior to the temporal vascular arcades at the insertion of the superior and inferior oblique muscles. On color fundus photography the SC lesions are white, placoid and irregular in appearance. On OCT, Hasanreisoglu et al. described the scleral involvement as irregular rather than smooth, with a “rocky” or “rolling” appearance.<sup>22</sup> On B-scan ultrasonography there is more shadowing of the lesion due to calcification. Finally, SC can be associated with systemic conditions linked to a disturbance in calcium-phosphorus metabolism.<sup>23, 24</sup> Another entity associated with scleral protrusion and choroidal thinning is “focal inferotemporal scleral bulge”, a non-pathologic finding likely associated with the insertion of the inferior oblique muscle.<sup>25</sup>



Initial findings on color fundus photography (CFP) and swept-source optical coherence tomography (SS-OCT) in the present case with sclerochoroidal calcification (SCC) secondary to chronic kidney disease (CKD). **a** CFP in the right eye showing pale choroidal lesions in the inferior mid-periphery (blue arrowheads). **b** CFP in the left eye showing a cluster of choroidal folds in the superotemporal extra-macular region (red arrows) and pale choroidal lesions in the superior regions (blue arrowheads). **c** SS-OCT in the right eye at vertical scans through the central fovea showing ellipsoid zone (EZ) disruption (yellow arrowhead) and dilated Haller layer veins, together with central choroidal thickness exceeding 300  $\mu\text{m}$  (green arrow). **d** SS-OCT in the left eye at vertical scans through the central fovea showing retinal pigment epithelium (RPE) undulation at the site of choroidal thinning due to scleral elevation (red circle). Dilated Haller layer veins were prominent together with central choroidal thickness exceeding 300  $\mu\text{m}$  (green arrow)



Initial findings on B-mode echography and orbital computed tomography (CT) in the present case with SCC secondary to CKD. **a** B-mode echography in the left eye at a vertical scan through the optic nerve showing hyperechoic lesions with acoustic shadowing (yellow circles). **b** Orbital CT at a coronal scan through the eye globes showing scleral high-density areas (red arrows)



Initial findings on fluorescein angiography (FA), indocyanine green angiography (ICGA), fundus autofluorescence (FAF), and laser speckle flowgraphy (LSFG) in the present case with SCC secondary to CKD. **a** FA showing hyperfluorescence (yellow circle) in the right eye. **b, c** ICGA showing choroidal vascular hyperpermeability (CVH) at the macular area together with numerous scattered hypofluorescent lesions (blue arrows) in both eyes and linear hyperfluorescent lesions (red arrows) in the left eye (**c**). **d** FAF in the right eye showing multiple hypoautofluorescent spots surrounded by hyperautofluorescent areas (yellow circle). **e, f** LSFG showing choroidal blood flow reduction represented by a colder color pattern in the right eye (**e**) than in the left eye (**f**)

# *Photo Essay*

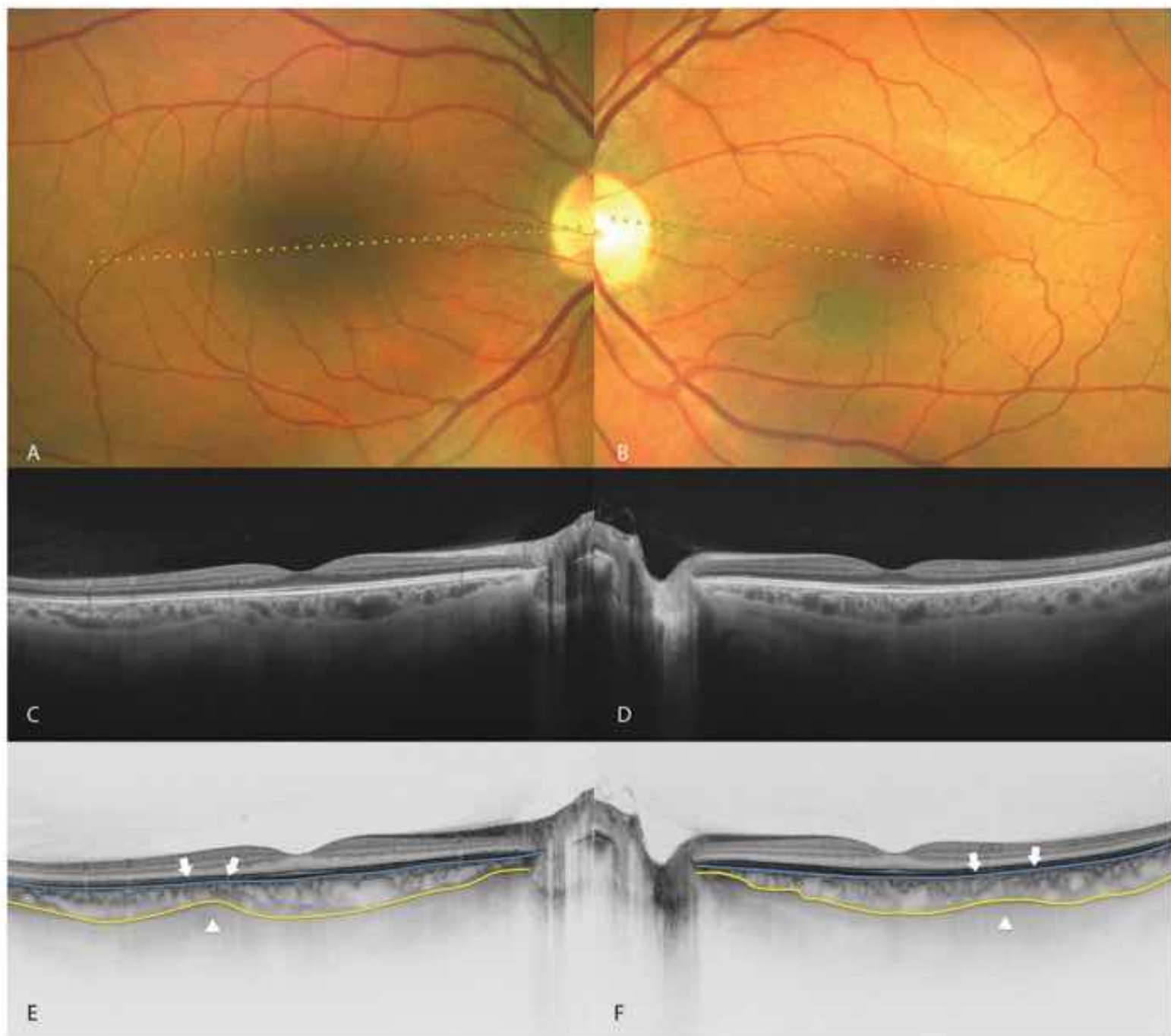
---

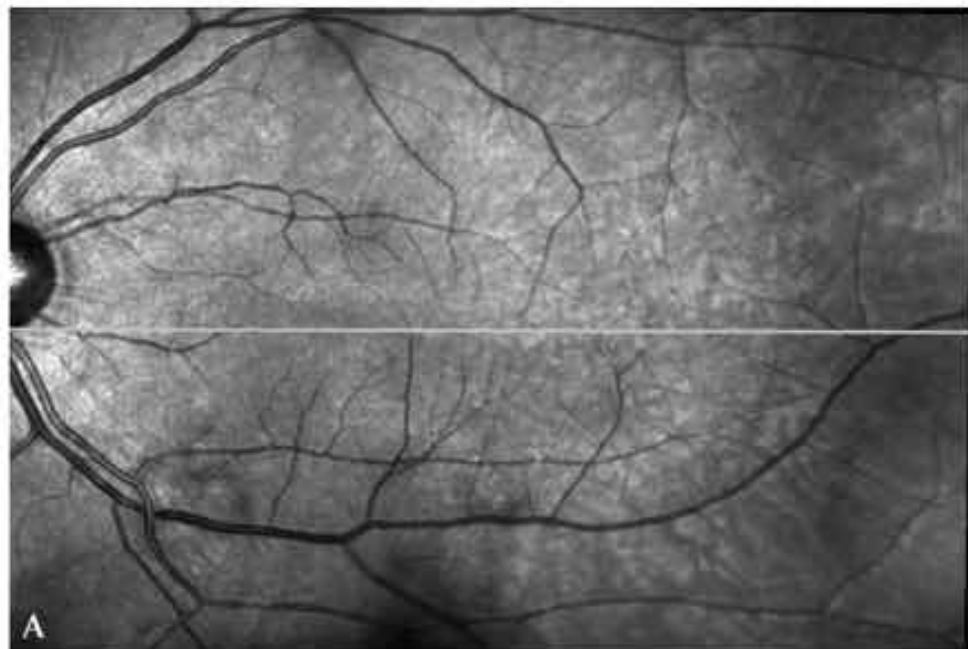
Edited by Cynthia A. Toth with Sumit Sharma and Dilraj S. Grewal

## **Focal Inferotemporal Scleral Bulge With Choroidal Thinning**

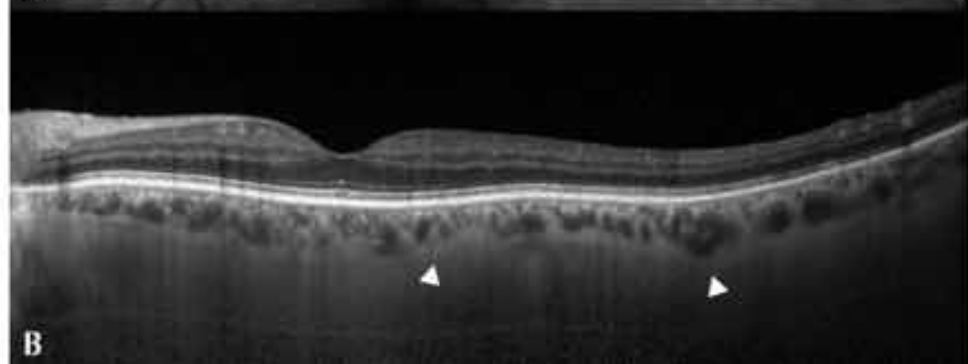
**A New Observation on High-Penetration Optical  
Coherence Tomography**

**Fig. 1.** A 36-year-old healthy woman. Color fundus photographs (A and B) show normal retinal appearance. Optical coherence tomography (C–F) displays focal inward bulge of the sclerochoroidal junction in the inferotemporal macular area in both eyes (arrowheads), with a related decrease in the overlying CT (arrows).





A



B

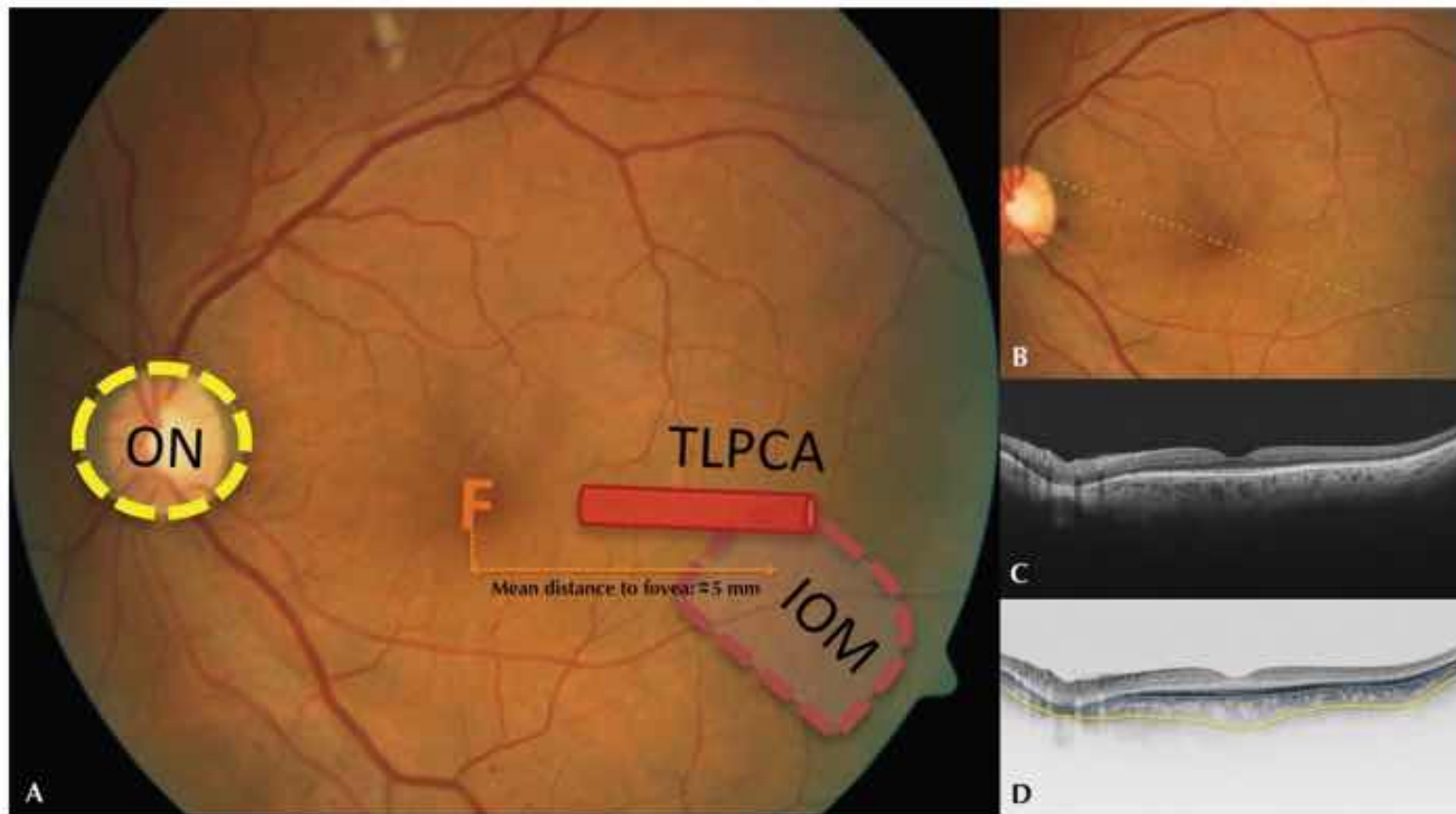


**Fig. 3.** A 59-year-old man with mild diabetic macular edema. The schema (A) shows the topographic location of the long posterior temporal ciliary artery (TLPCA) and the inferior oblique muscle (IOM) overlapped to the color fundus photograph, adapted from Reference 5. Color fundus photographs (B) evidence nonproliferative diabetic retinopathy in the left eye. Optical coherence tomography (C–D) shows mild foveal thickening. The sclerochoroidal junction exhibits a focal temporal inward bulge (arrowheads), with a concomitant thinning of overlying choroid (arrows).

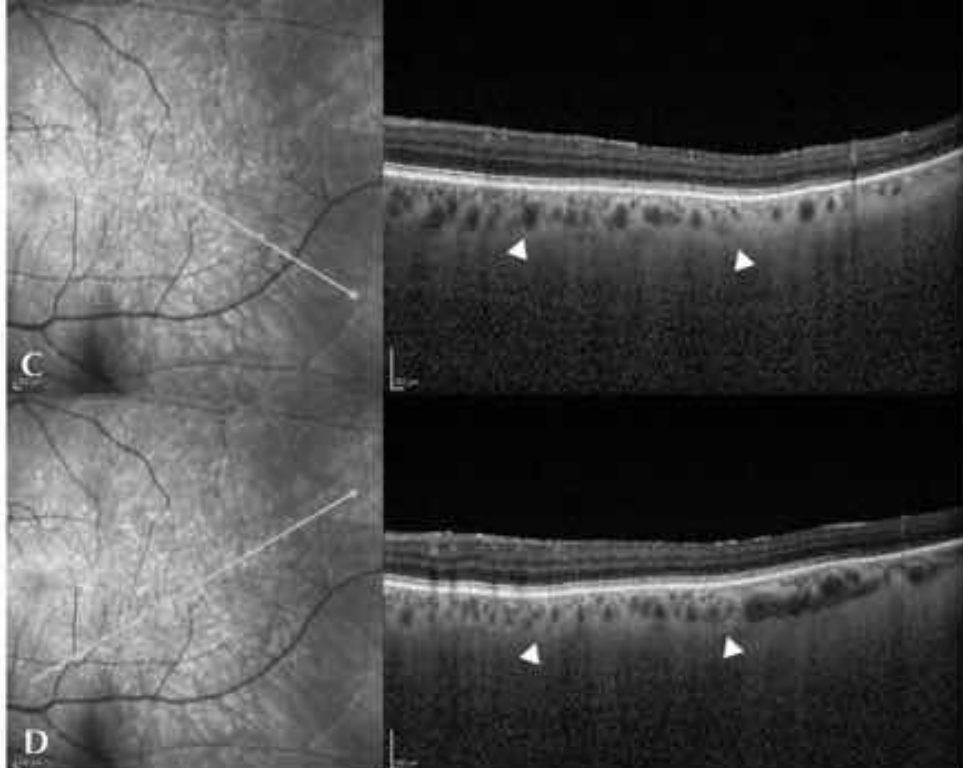


**Fig. 2.** A 50-year-old healthy man. The infrared fundus image (A) shows an unremarkable appearance. Optical coherence tomography horizontal scan (B) centered in the fovea exhibits a focal temporal inward bulge of the sclerochoroidal edge (arrowhead) and a focal decrease in the CT underlying a normal retina. The scleral bulge appears independent of the optical coherence tomography scan angle (C–D).

PHOTO ESSAY | VOLUME 55, ISSUE 5, P466-467, OCTOBER 2020

 Download Full Issue

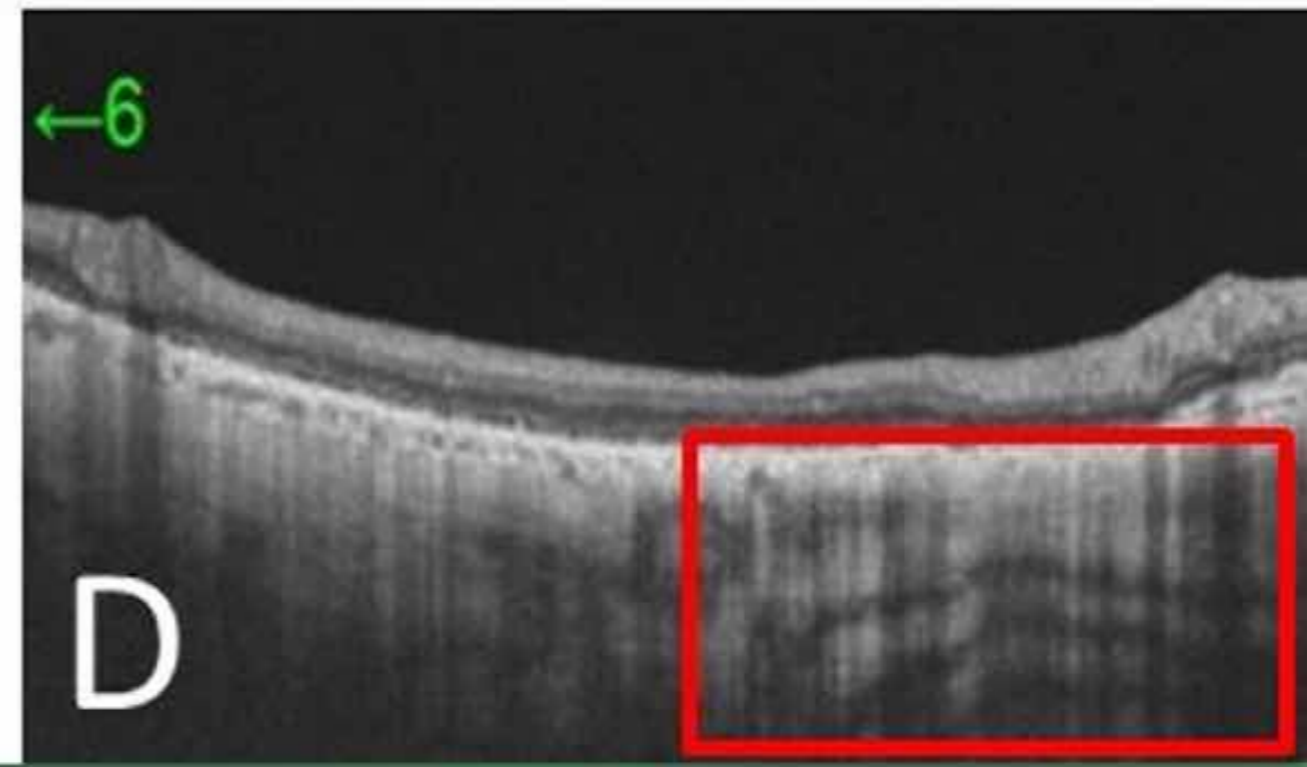
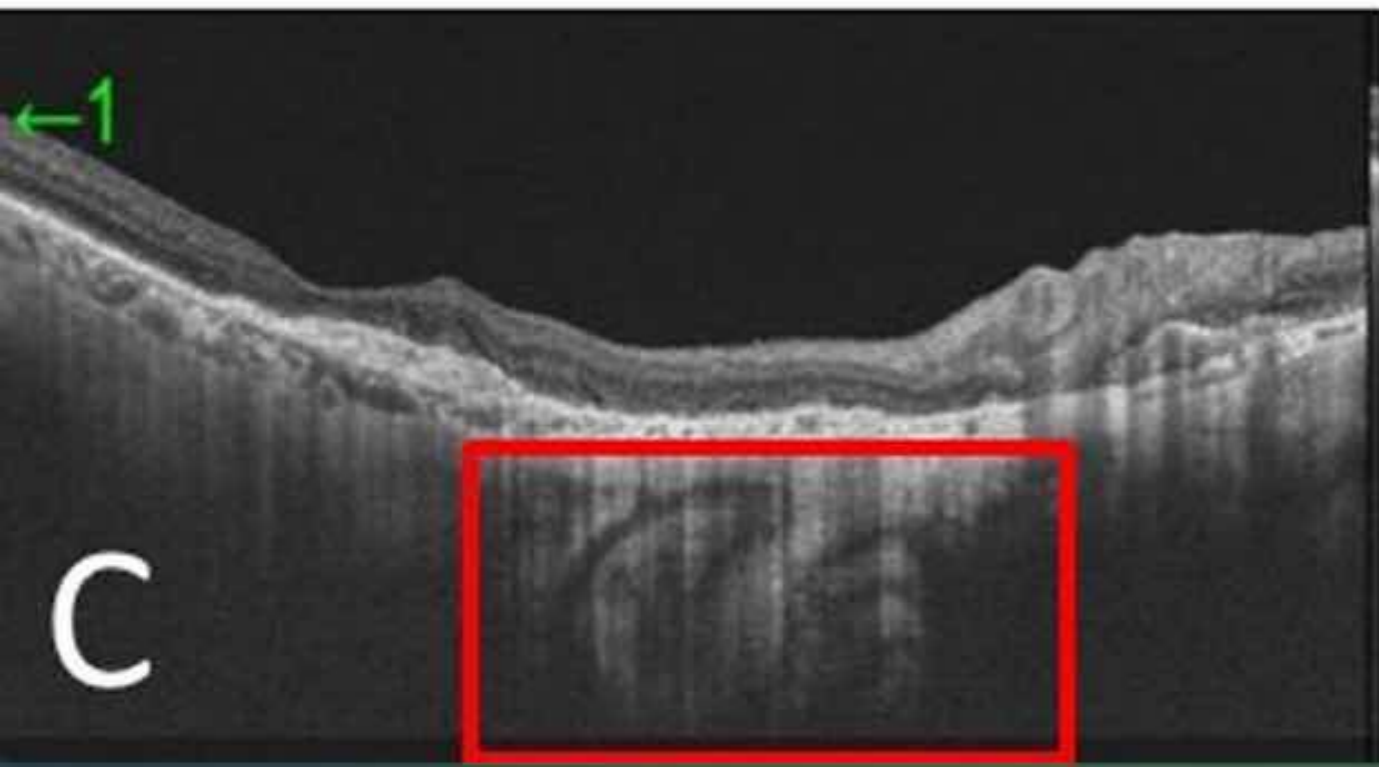
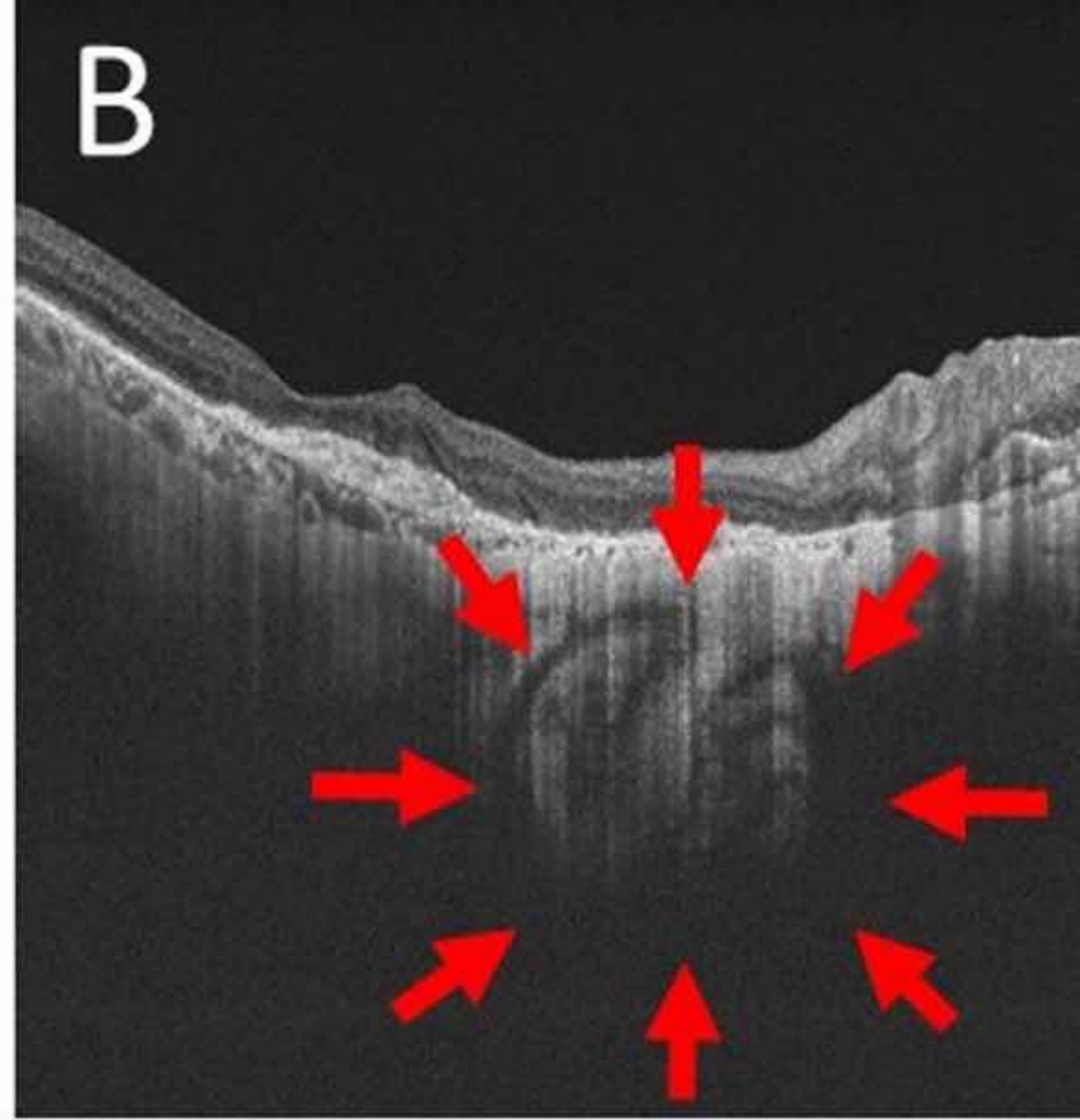
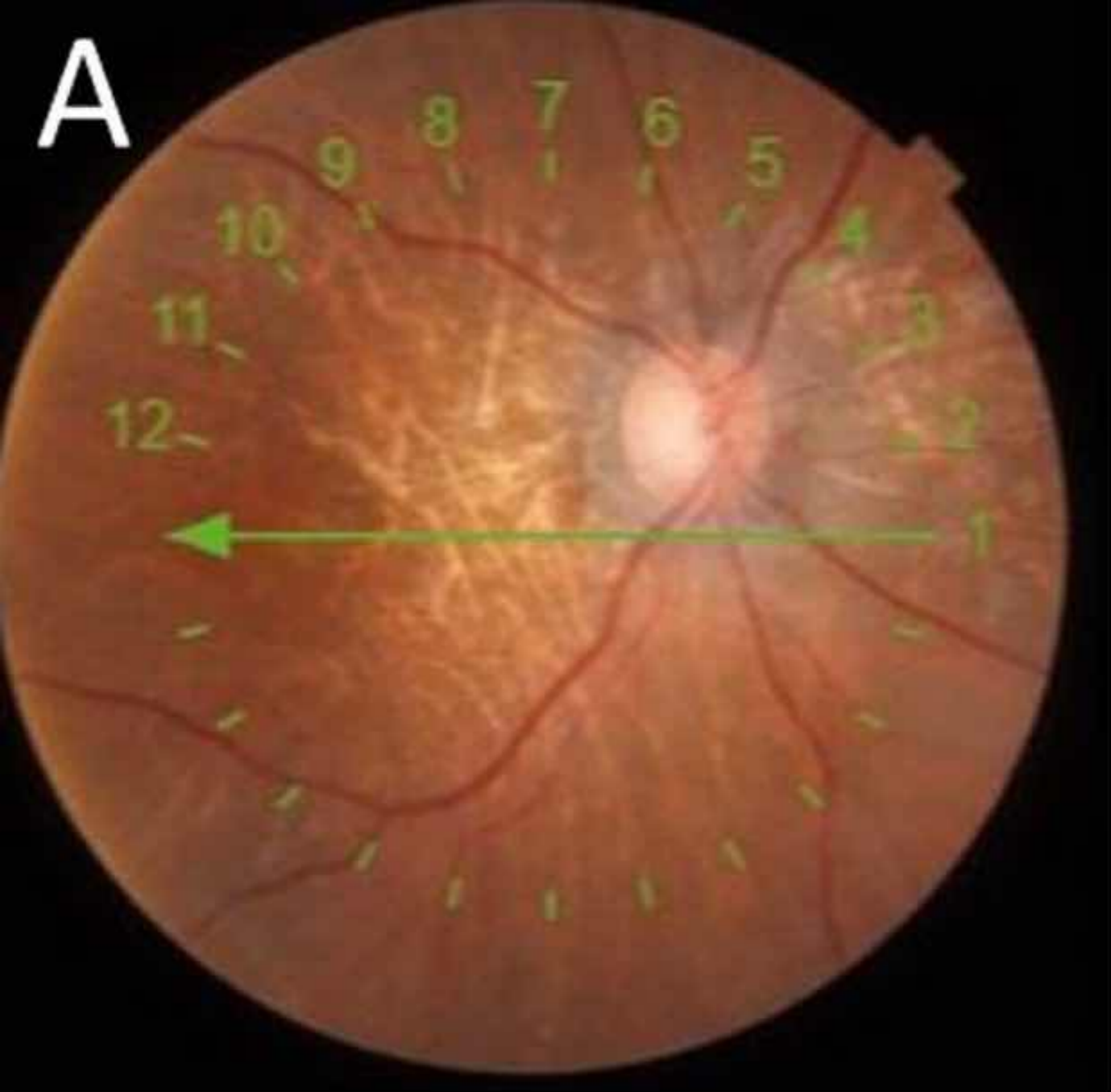
# Imaging the inferior oblique using optical coherence tomography

[Julio González-Martín-Moro, MD, PhD](#)   • [Fernando Gomez-Sanz](#) • [Inés Contreras, MD, PhD](#)

Published: June 07, 2020 • DOI: <https://doi.org/10.1016/j.jcjo.2020.04.021> •



Check for updates



An 81-year-old woman presented for a routine follow-up of her dry age-related macular degeneration (Fig. 1A). She had normal eye balance and no history of strabismus. Optical coherence tomography (OCT) radial scan, using Triton OCT (Topcon, Tokyo, Japan), showed a round area behind the sclera, slightly inferior to the macula in her right eye (Fig. 1B, 1C). The vertical cuts (Fig. 1D) showed its fascicular organization. The morphology and position suggest that this structure was the inferior oblique muscle. This is probably the first report on the potential of OCT to visualize the inferior oblique muscle in patients with severe chorioretinal atrophy.